Human Tolerance Research Program

Vehicle
Research
Institute

vehicle research
institute report
VRI 8.2

SOCIETY OF AUTOMOTIVE ENGINEERS, INC.

UM-HSRI-BI-74-3

HUMAN TOLERANCE RESEARCH PROGRAM

First Year Interim Report

Richard L. Stalnaker
John W. Melvin
Biosciences Division
Highway Safety Research Institute
The University of Michigan
Ann Arbor, Michigan 48105

Report To:

Vehicle Research Institute
Society of Automotive Engineers

HIGHWAY SAFETY RESEARCH INSTITUTE
Institute of Science and Technology
Huron Parkway and Baxter Road
Ann Arbor, Michigan 48105

THE UNIVERSITY OF MICHIGAN

March 24, 1975

Mr. John Scowcroft
Motor Vehicle Manufacturers Association
320 New Center Building
Detroit, Michigan 48202

Dear Mr. Scowcroft:

Enclosed please find 50 copies of the VRI first year report "Human Tolerance Research Program." The remaining 50 copies have been sent to Mr. Toth of SAE.

If you have any questions, please do not hesitate to contact me.

Sincerely,

Richard L. Stalnaker, Ph.D.
Assoc. Research Engineer
Biomechanics Department

RLS:kps

HIGHWAY SAFETY RESEARCH INSTITUTE
Institute of Science and Technology
Huron Parkway and Baxter Road
Ann Arbor, Michigan 48105

THE UNIVERSITY OF MICHIGAN

March 24, 1975

Mr. William Toth
Society of Automotive Engineers
400 Commonwealth Drive
Warrendale, Pennsylvania 15096

Dear Mr. Toth:

Enclosed please find 50 copies of the VRI first year report, "Human Tolerance Research Program." The remaining 50 copies have been sent to Mr. Scowcroft of MVMA.

If you have any questions, please do not hesitate to contact me.

Sincerely,

Richard L. Stalnaker, Ph.D.
Assoc. Research Engineer
Biomechanics Department

RLS:kps

1. Report No.	2. Government Accession No.	3. Recipient's Catalog No.
UM-HSRI-BI-74-3		

4. Title and Subtitle	5. Report Date
Human Tolerance Research Program First Year Interim Report	6. Performing Organization Code September 1974
7. Author(s) Stalnaker, Richard L. Melvin, John W.	8. Performing Organization Report No. UM-HSRI-BI-74-3
9. Performing Organization Name and Address Highway Safety Research Institute The University of Michigan Huron Parkway & Baxter Rd. Ann Arbor, Michigan 48105	10. Work Unit No. 11. Contract or Grant No.
12. Sponsoring Agency Name and Address Vehicle Research Institute	13. Type of Report and Period Covered First Year Interim 4-15-73 to 5-15-74 14. Sponsoring Agency Code

15. Supplementary Notes

16. Abstract

This interim report discusses the progress during the first year of a two year program on advanced research in human tolerance to impact. The areas of interest in the program are the determination of the following:

1. Relationships between linear and angular impacts of various intensity and direction to the head and the resulting injuries.
2. Effective principal moments of inertia of the head in rotation.
3. Tolerance of the femur to longitudinal and transverse impact.
4. Tolerance of the tibia and fibula to transverse impact.

The test subjects used in this program are all unembalmed human cadavers. A unique feature of the program is the use of sufficient instrumentation to determine the three dimensional motion of the head both during impact and in the motion that follows. In order to accomplish this, many special techniques had to be developed, and the appropriate test fixtures had to be designed and built. The details of these techniques and fixtures are found in the Appendices of this report. The advantage of such complete instrumentation is that the data on head motion produced in each test can be reduced to give the linear and angular accelerations of any point within the head and can be recalculated at a different point at a later date if so desired. This report discusses the experimental techniques developed for the various tasks of the program and presents the results of preliminary tests performed during the first year of the program.

17. Key Words	18. Distribution Statement

19. Security Classif.(of this report)	20. Security Classif.(of this page)	21. No. of Pages	22. Price

Form DOT F 1700.7 (8-69)

TABLE OF CONTENTS

TABLE OF CONTENTS (Continued)

LIST OF FIGURES

LIST OF FIGURES (Continued)

1.0 INTRODUCTION

With the advent of high-speed air and land transportation, engineers have become increasingly aware of the mechanical frangibility of the human body. Thus we have seen the evolution of various isolating and load-distributing devices ranging from seat belts and padded sun visors to ejection seats, crash helmets, and acceleration couches. While there is a large amount of information available regarding the response of inanimate systems to vibration and impact, there is a comparable dearth of knowledge pertaining to the mechanical response of biological systems. Therefore, the design of much supporting and protective equipment is often based on intuition because of the lack of available information about the mechanical behavior of the human body. In addition, such knowledge would be helpful in the treatment of injury by serving to identify the mechanism of trauma. Thus, both a rational design procedure for impact protection and a rational therapy for treatment of trauma cannot be developed until a quantitive description of the mechanical responses of the human body is obtained.

Significant progress in human tolerance research in the past has been impeded by the lack of suitable experimental subjects. Various models of man have been used to study his response to external forces and to document his limitations. These have included various species of subhuman primates ranging from the squirrel monkey to the chimpanzee, bears, embalmed human cadavers, and human volunteers. The limitations of each choice of test subject have become apparent, particularly after the resulting experimental data have been applied to the living human in a crash environment.

In this program it was proposed to use unembalmed human cadavers to study head and leg tolerance to direct impact. The following specific tasks were set to be accomplished in the program:

(1) Determine the relationship between impacts of varying intensity and injury for blows applied to the head. Blows will be directed at the front, rear, and oblique sites to determine the dependence of injury on impact direction.

(2) Determine the effective dynamic moments of inertia in torsion for the three principal axes.

(3) Conduct head impacts in a torsion-only mode to relate head injury to impact intensity.

(4) Determine the human tolerance of the patella and femur system for impacts in the long axis of the femur. Determine the tolerance of the femur to lateral impact.

(5) Determine the tolerance of the tibia and fibula to impact applied normal to the lower leg from the front and side.

This is a final report on the first year of a two-year project. The thrust of the first year was on the development of the test procedures to be used in the completion of the project in the second year.

Due to the large number of tests proposed in this study, it became obvious that a revision of old test procedures would have to be undertaken. It was decided for maximum efficiency that as many tests as possible should be run on the same cadaver. To implement this decision, all of the test procedures and fixtures were redesigned and constructed. This revision makes it possible to bring in a cadaver and perform tasks 1 through 5 in a 24-hour period. This means that better cadaver material can be used in these tests. The following is a detailed description of the test fixtures and some procedures that are to be used in the second year.

A unique feature of the program is the use of sufficient instrumentation to determine the three-dimensional motion of the head both during impact and in the motion that follows. In order to accomplish this, many special techniques had to be developed, and the appropriate test fixtures had to be designed and built. The details of these techniques and fixtures are found in the Appendices of this report. The advantage of such complete instrumentation is that the data on head motion produced in each test can be reduced to give the linear and angular accelerations of any point within the head and can be recalculated at a different point at a later date if so desired. Thus, the data produced in the program will be of use to future studies without the usual restriction of limited data (such as triaxial linear accelerations only at a specific point) that past studies have produced.

2.0 METHOD

2.1 Task I

The specimens used in this study are fresh, unembalmed cadavers obtained from the Anatomy Department of the University of Michigan Medical School. They are stored at 37° F for two of the three days between time of death and impact. The cadavers are transported to HSRI and allowed to reach room temperature before testing. This ensures that the effects of rigor mortis have disappeared and the blood is again fluid.

2.1.1 A-P Impacts

The axis of the impactor is in the mid-sagittal plane and is normal to the surface of the skull at the point of initial impact. The cadaver is positioned so that the inferior aspect of the six-inch diameter impactor is adjacent to the glabella and therefore no part of the impactor comes in contact with the subject's nose. The point of impact is located three

inches superior to the glabella in the mid-sagittal plane, or at the back of the occipital bone. This allows the impactor to contact the forehead in such a way as to load upon as large and flat a surface as possible.

The targets used for photographic analysis are in a plane extending in the L-R direction, common to the axis of impact. They are located two inches anterior and one inch posterior to the intersection of a line perpendicular to the axis of impact passing through the external acoustic meatus, with the above described plane. All targets are mounted on small wood screws, which are then driven into the skull (Figure 1a). The Class 1000 frequency response values for filtering were used for all head acceleration, as recommended by SAE Standard J211.

The accelerometer configuration attached to the head is that of three biaxial accelerometers located according to the analysis given in Appendix A. This array allows the complete determination of the three dimensional motion of the head as outlined in the flow chart shown in Figure 2.

After being targeted, x-rayed, and equipped with accelerometers as detailed in Appendix A, the cadaver is placed in a chair specially designed and constructed for this impact study (See Appendix B). All surfaces against which the cadaver might come in contact in its post-impact movements are thickly padded with styrofoam to prevent damage to the cadaver. A special foam apparatus is employed to absorb the energy of the head and to protect the accelerometers from damage.

The cadaver is carefully positioned so that its head is in the correct position relative to the impactor and at the same time the whole cadaver acts as a free body.

The head is suspended and held in place by four strands of 000 thickness surgical thread. This thread supports only the weight of the head, and

breaks easily on impact. The impacts were carried out in the HSRI Impact Facility.

Two kinds of impacting surfaces are used. The first surface is a six-inch diameter rigid metal disc. The second surface consists of the same metal disc with three inches of polystyrene foam (density = 1.78 lb/ft^3), fixed to the contacting surface of the disc to pad the impact.

Pre-impact travel of the impact piston is 1.5 inches for both padded and unpadded impactors. The post-impact travel is five inches for the padded impactors and three inches for the unpadded impactors. At the end of this travel, its motion is arrested mechanically and the cadaver head and torso continue their motion unimpeded.

2.1.2 L-R Impacts

The point of impact is the left temporal region, two inches superior to the external acoustic meatus. The photographic targets for L-R head impacts are located on the supra-orbital ridge, two inches on either side of the glabella (i.e., two inches either side of the mid-sagittal plane). The location of the targeting for side impacts is shown in Figure 1b. All other conditions for side impact are the same as indicated in Section 2.1.1.

2.2 Task 2 - Determination of the Effective Moment of Inertia of the Head of Intact Cadavers

The following test procedure has been developed for the estimation of the effective moment of inertia of the head of intact cadavers. Since intact cadavers will be used, the effective moment of inertia will be measured along an axis passing through the center of gravity of the head. The term "effective" is used since the measurements will be influenced by the head torso linkage.

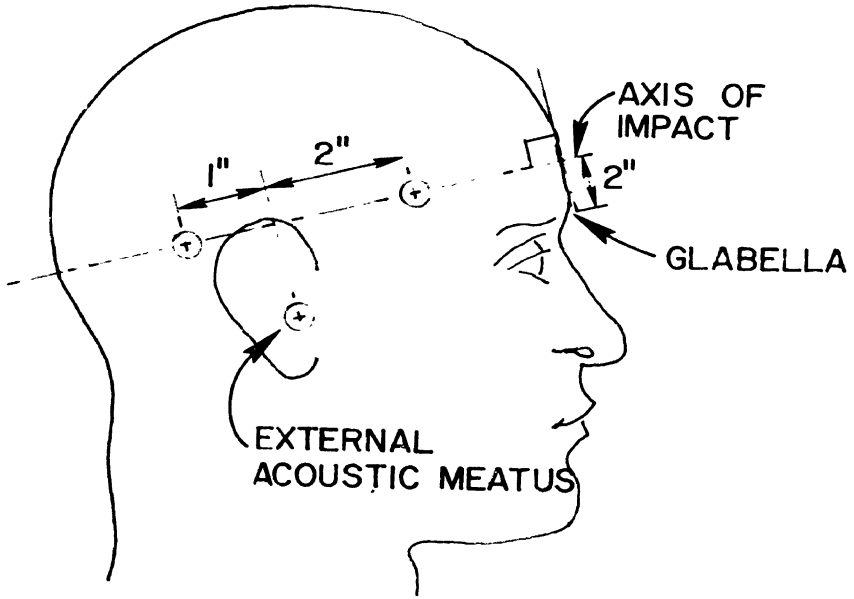

FIGURE 1(a). TARGETING FOR FRONT AND BACK HEAD IMPACTS.

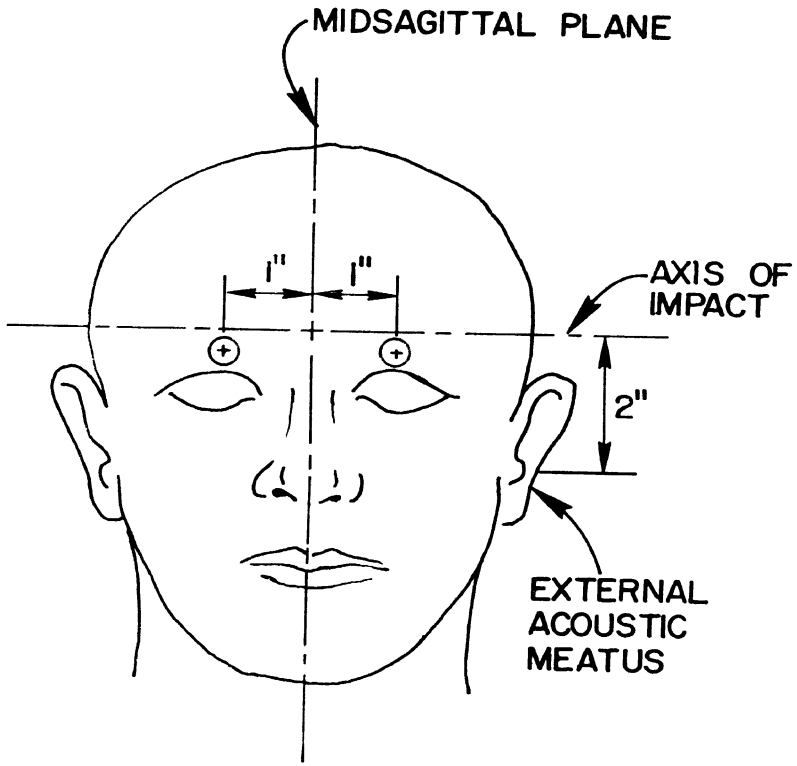

FIGURE 1(b). TARGETING FOR SIDE HEAD IMPACTS.

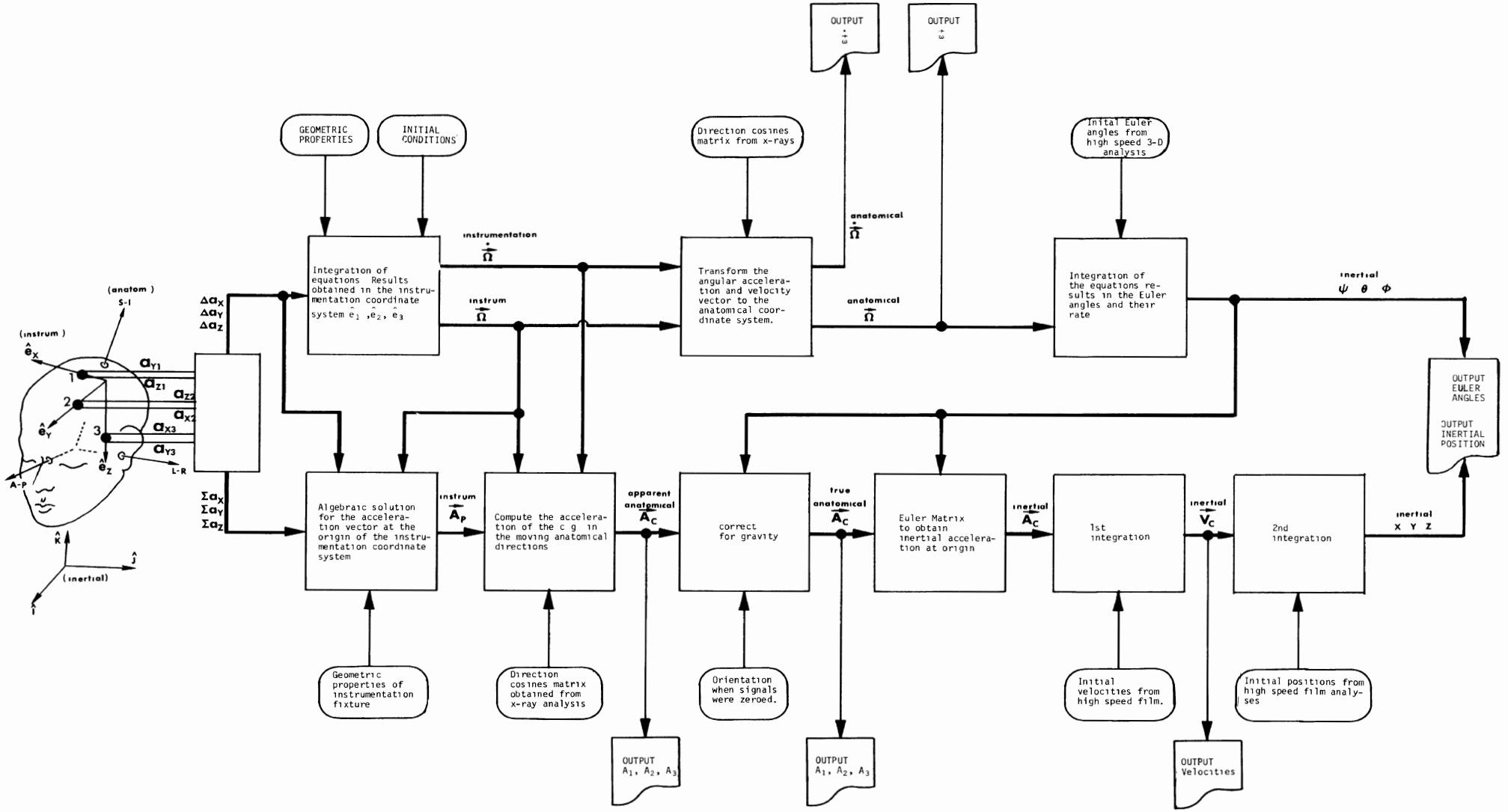

FIG 2: RIGID-BODY HEAD-MOTION ANALYSIS PROCEDURE FLOW DIAGRAM

2.2.1 Anthropometric Measurements and Location of C.G. of the Head

Fresh unembalmed cadavers obtained from the Anatomy Department of The University of Michigan Medical School will be used in the study. Usually the cadavers are stored at 37° F from one to seven days before the test is carried out. The specimens will be allowed to reach room temperature before any tests are carried out.

The coordinate system to be used is indicated in Figure 3. The origin is at the mid point of a line connecting the superior edges of the right and left auditory meati (1).* The +X axis is from the origin to the midpoint of a line connecting the infraorbital notches in the anatomical plane. The following anthropometric measurements will be made of each specimen (See Figure 4).

1. Head Length: Maximum length of the head between the glabella landmark and the occiput (mid-sagittal plane).
2. Head Breadth: Maximum horizontal breadth above the level of the ears.
3. Tragion to Vertex Height.
4. Circumference: Above the brow ridges and parallel to the Frankfort plane.
5. Effective Weight.

When the center of gravity locations are expressed in the head anatomical coordinate system, it is seen that they do not vary a great deal (1). For purposes of standardization, we will assume the location of C.G. to be as follows:

$\overline{X}$ = + 1.1 cm

$\overline{Z}$ = + 2.1 cm

* Numbers in parentheses denote references at the end of the text.

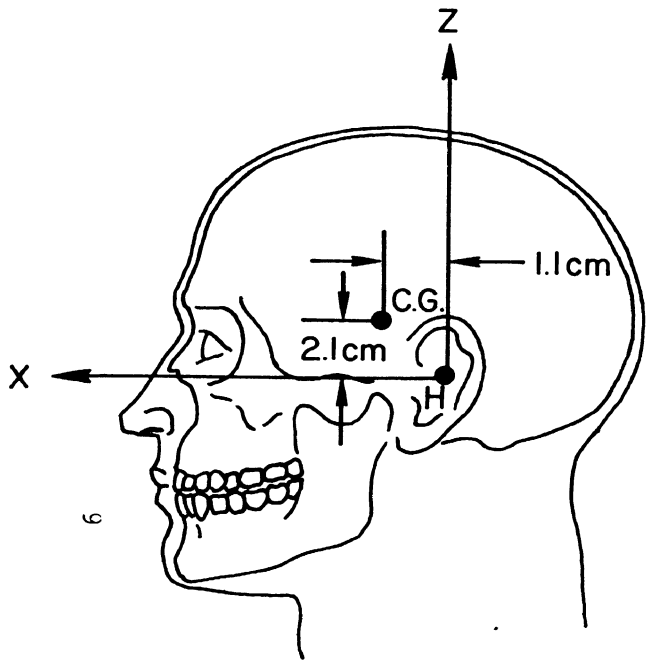

H = Head anatomical co-ordinate system

C.G. = Center of gravity of head

FIGURE 3

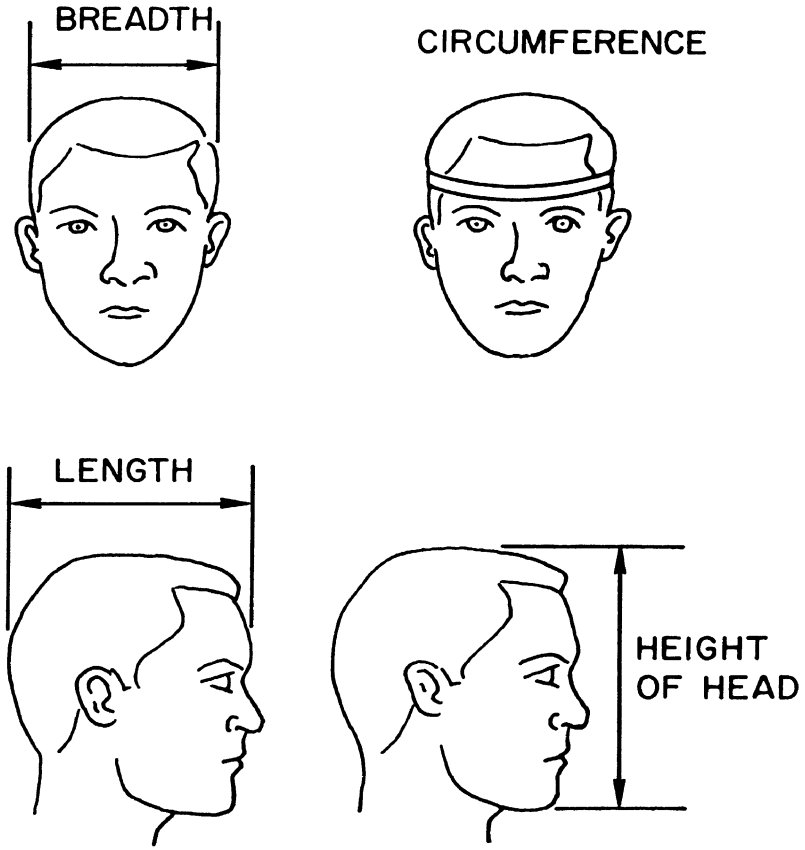

FIGURE 4

2.2.2 Location of Rotational Axes in the A-P, L-R, and S-I Directions with Origin at C.G.

A special axis-location device (Figure 5) has been designed which will be used to locate points on the surface of the head through which the axes of rotation will pass if the head is rotated in the XY, XZ, and YZ planes with the C.G. as the origin. This device will be placed so that the hole O is over the superior edges of the auditory meati and EF along the infra-orbital notches. The point G is 1.1 cm and 2.1 cm from O in the +X and +Y directions. This point will be marked on the head at both sides of the head. Mid-points of AB, CD, and EF will give the other points which will be similarly marked on the skull.

2.2.3 Determination of the Effective Moment of Inertia

An MTS Systems Torsional Shaker will be used to shake the head. The shaker will be calibrated dynamically by mounting an aluminum cylinder of known moment of inertia (250000 gm-cm^2, approximately the same as that of the head about the y axis). By shaking the cylinder at a known frequency and pulse shape (sinusoidal), the torques can be calculated at different frequencies:

$$T = I\ddot{\theta}$$

where T is the torque, I the moment of inertia, and $\ddot{\theta}$ the angular acceleration.

The cadaver body will be placed on a special table which can be raised or lowered so as to position the head in the desired place over the shaker head. The head will then be aligned in the fixture (Figure 6) which has been specially designed for this purpose, so that the axis of rotation passes through the assumed center of gravity. This will be done with the help of the surface landmarks already determined. Then the three screws A, B, and

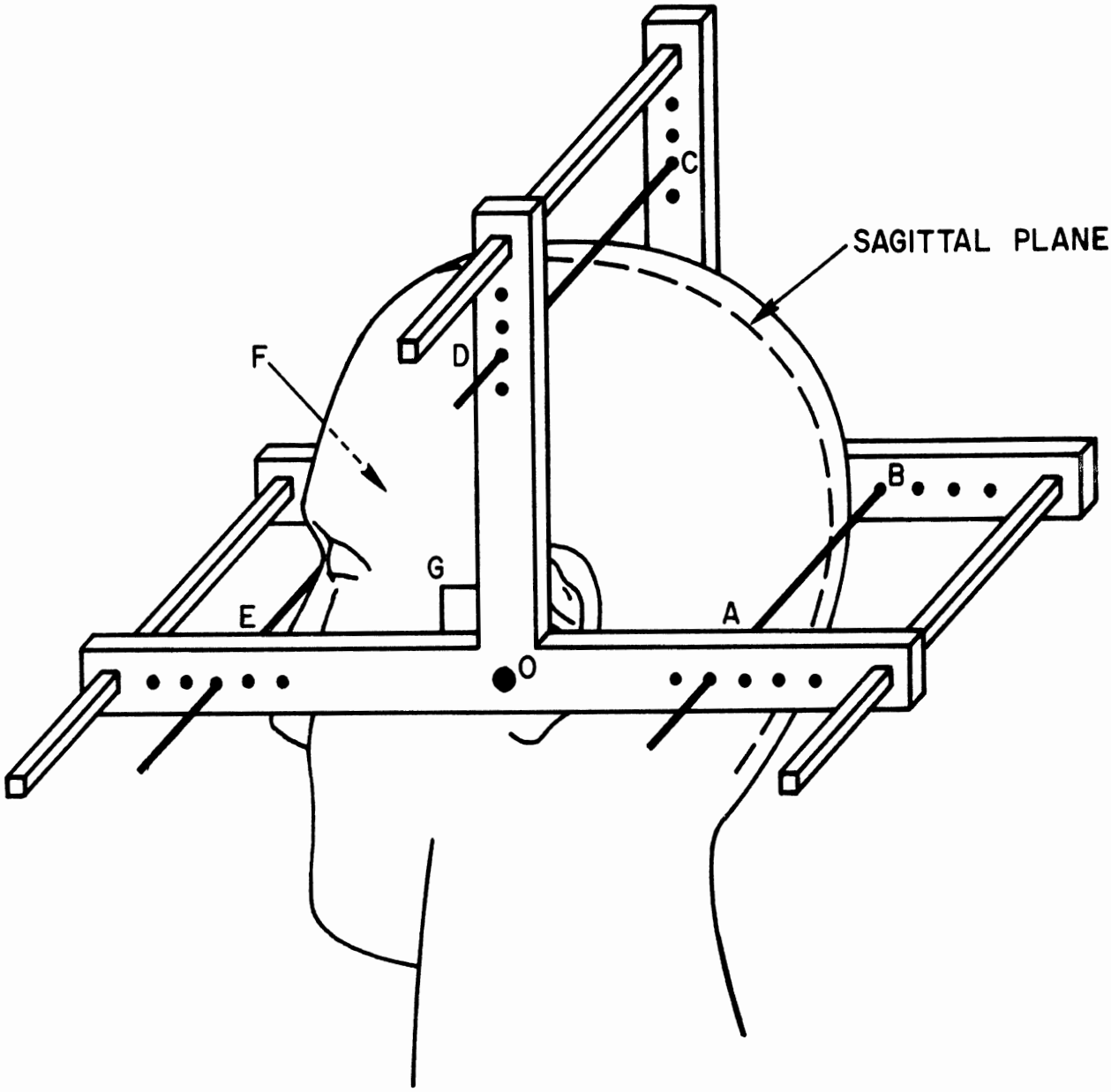

FIGURE 5.

DEVICE FOR LOCATING

SPECIAL AXES

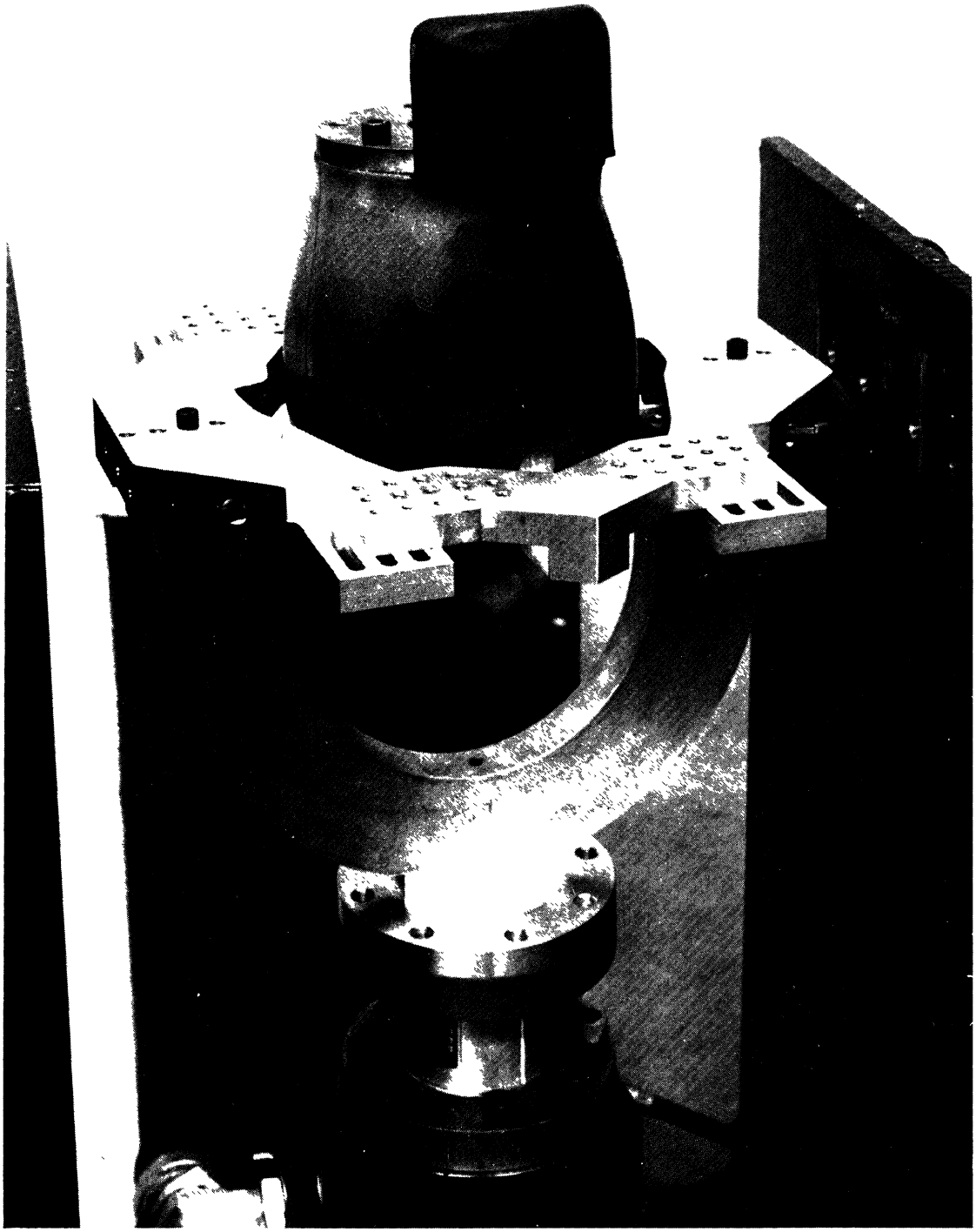

FIGURE 6. HEAD MOMENT OF INERTIA TEST SET-UP

C will be screwed into the skull to hold it in place. To reduce the load on the screws, thin aluminum plates will be screwed into the fixture and then quick-setting rigid foam injected in the cavity so formed. Once the foam hardens, the head will be secured in place.

The head will then be vibrated on the torsional shaker and the frequency, pulse shape, and torque values recorded. With this information, the effective moment of inertia for the head system fixture can be calculated. The head will then be removed and a similar test run for the fixture with the foam, With these values known, the effective moment of inertia of the head can then be obtained. The moment of inertia in the other two directions will then be determined by reorienting the head in the desired direction. Since the structural integrity of the head is not violated in the test procedure, it is possible to conduct many tests on the same head in this manner. The moment of inertia about any other axis can then be determined.

2.3 Task 3

In this task, a single-shot triangular displacement pulse at varying amplitudes and time durations will be used as input to the head. In this series of tests the head will be fastened to the hydraulic torsional shaker in the exact manner as described in Task 2.

2.4 Tasks 4 and 5

The cadaver for these tests will be placed in the chair as described in Task 1. Impacts to the patella and femur system along the long axis of the femur will be made with a five-inch-diameter padded impactor. Impacts to the side of the femur will be delivered by a six-inch-diameter cylinder. In both of these tests, impacts will be repeated until fracture is obtained.

In Task 5 the impacts to the tibia and fibula will be conducted using the six inch cylinder as described in the above paragraph.

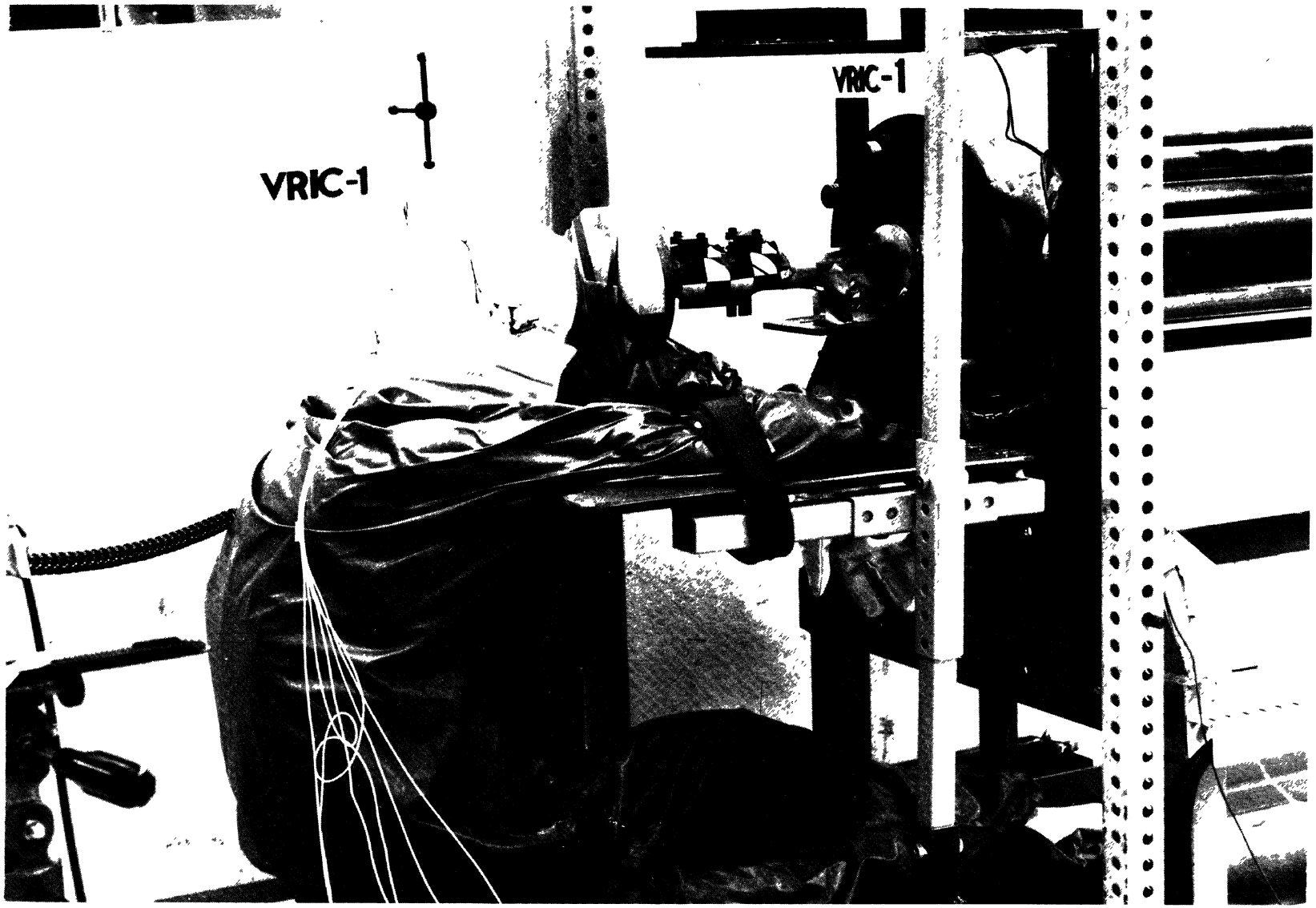

FIGURE 7. TEST SET-UP FOR HEAD IMPACTS

IMPACT FORCE VS. TIME FOR VRIC-1

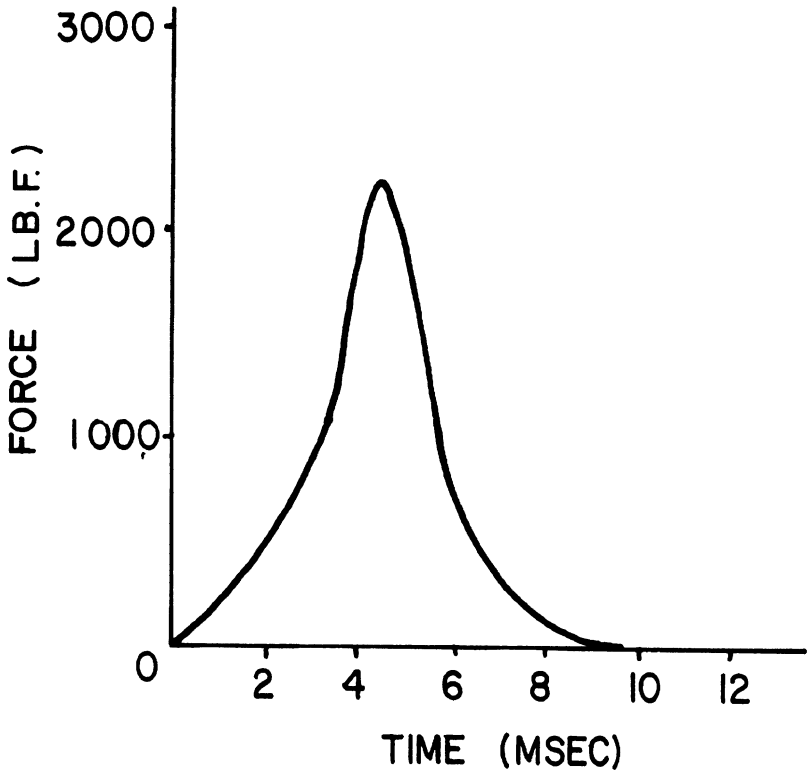

FIG. 8

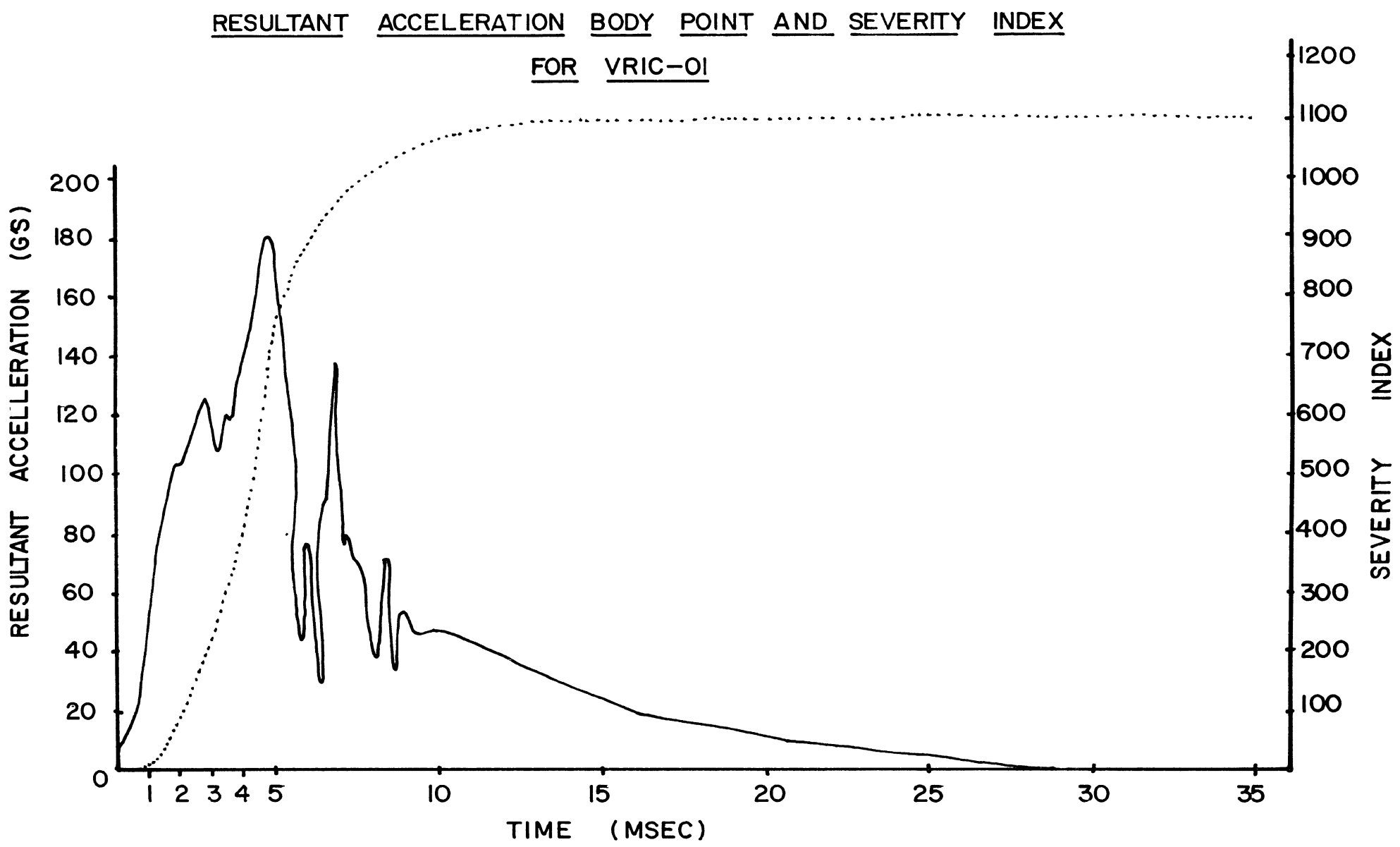
RESULTANT ACCELERATION BODY POINT AND SEVERITY INDEX
FOR VRIC-01
RESULTANT ACCELLERATION (GS)
SEVERITY INDEX
TIME (MSEC)
0
20
40
60
80
100
120
140
160
180
200
100
200
300
400
500
600
700
800
900
1000
1100
1200
1
2
3
4
5
10
15
20
25
30
35

FIG. 9

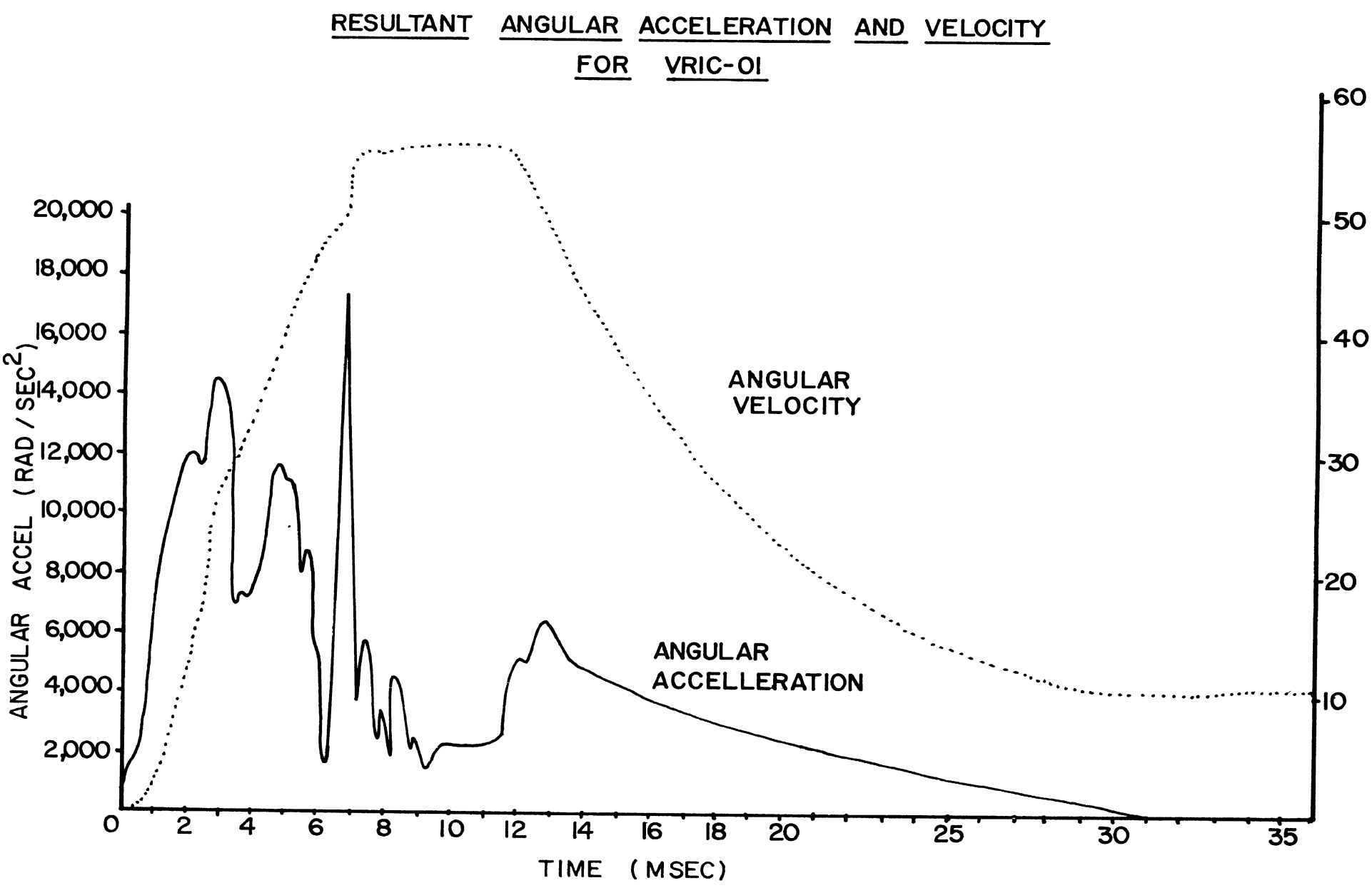
RESULTANT ANGULAR ACCELERATION AND VELOCITY
FOR VRIC-01
ANGULAR ACCEL (RAD/SEC²)
20,000
18,000
16,000
14,000
12,000
10,000
8,000
6,000
4,000
2,000
0
2
4
6
8
10
12
14
16
18
20
25
30
35
TIME (MSEC)
60
50
40
30
20
10
ANGULAR VELOCITY
ANGULAR ACCELLERATION

FIG. 10

YAW AND YAW RATE OF BODY POINT FOR VRIC — 01

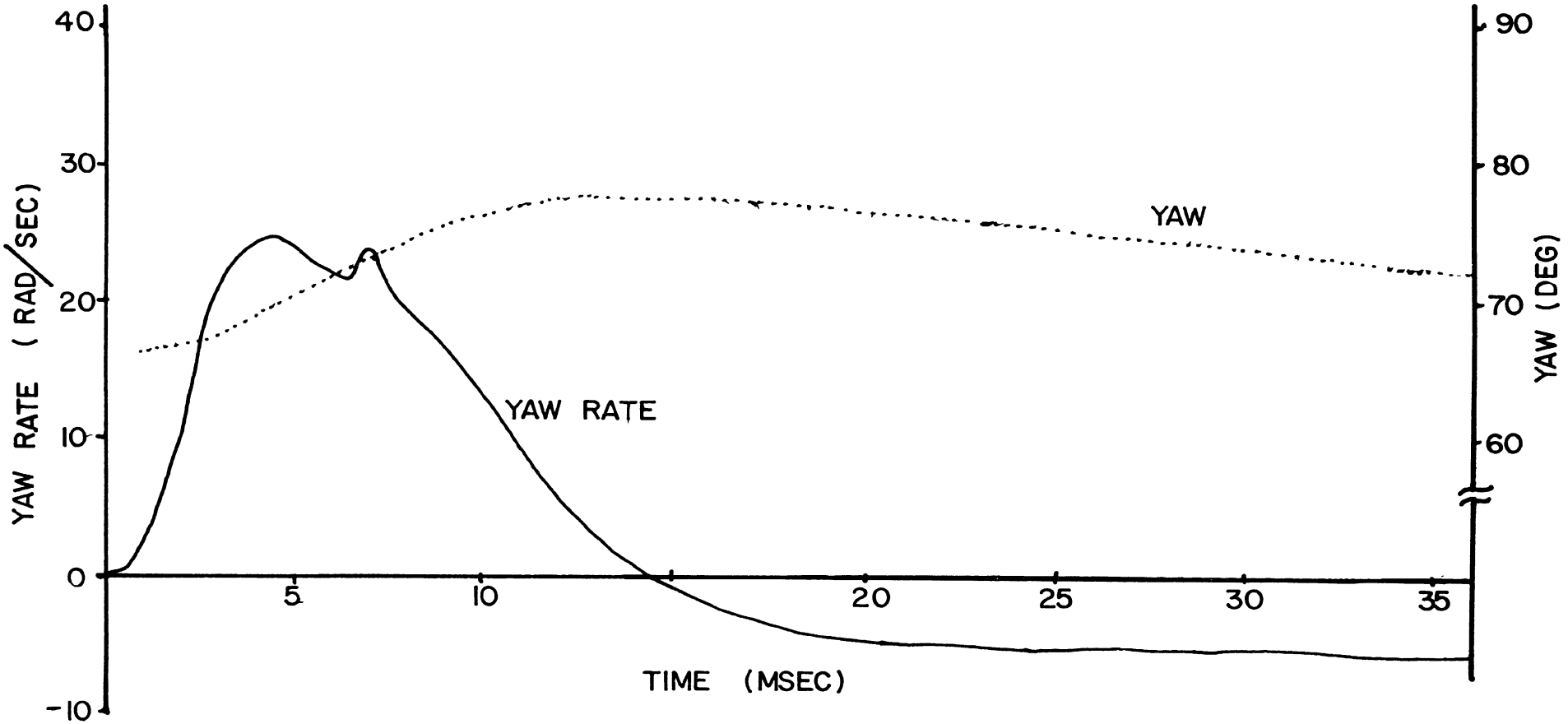

FIG. 11

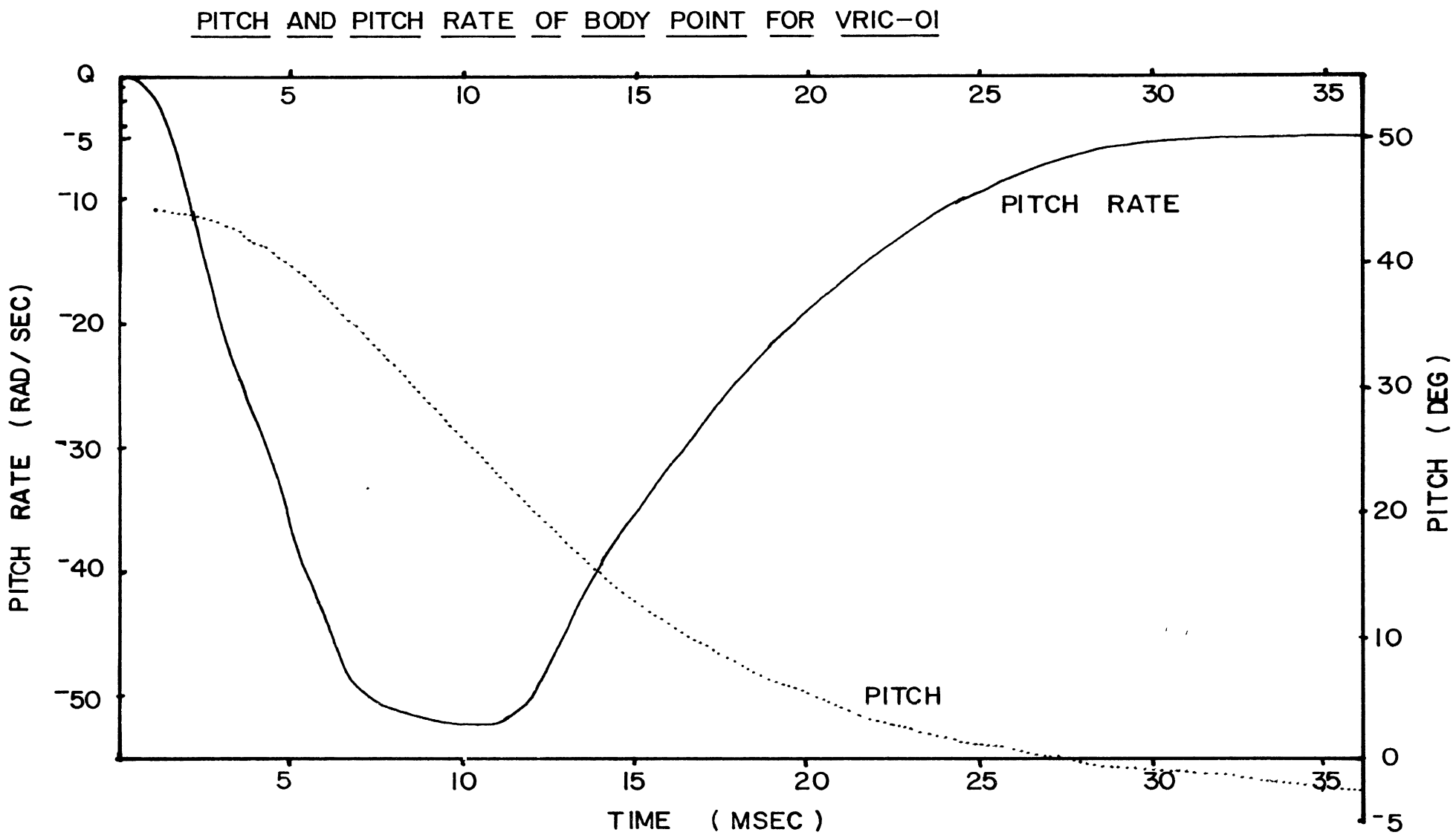
PITCH AND PITCH RATE OF BODY POINT FOR VRIC-01
PITCH RATE (RAD/SEC)
PITCH (DEG)
TIME (MSEC)
PITCH RATE
PITCH
0
-5
-10
-20
-30
-40
-50
5
10
15
20
25
30
35
50
40
30
20
10
0
-5

FIG. 12

ROLL AND ROLL RATE OF BODY POINT FOR VRIC-01

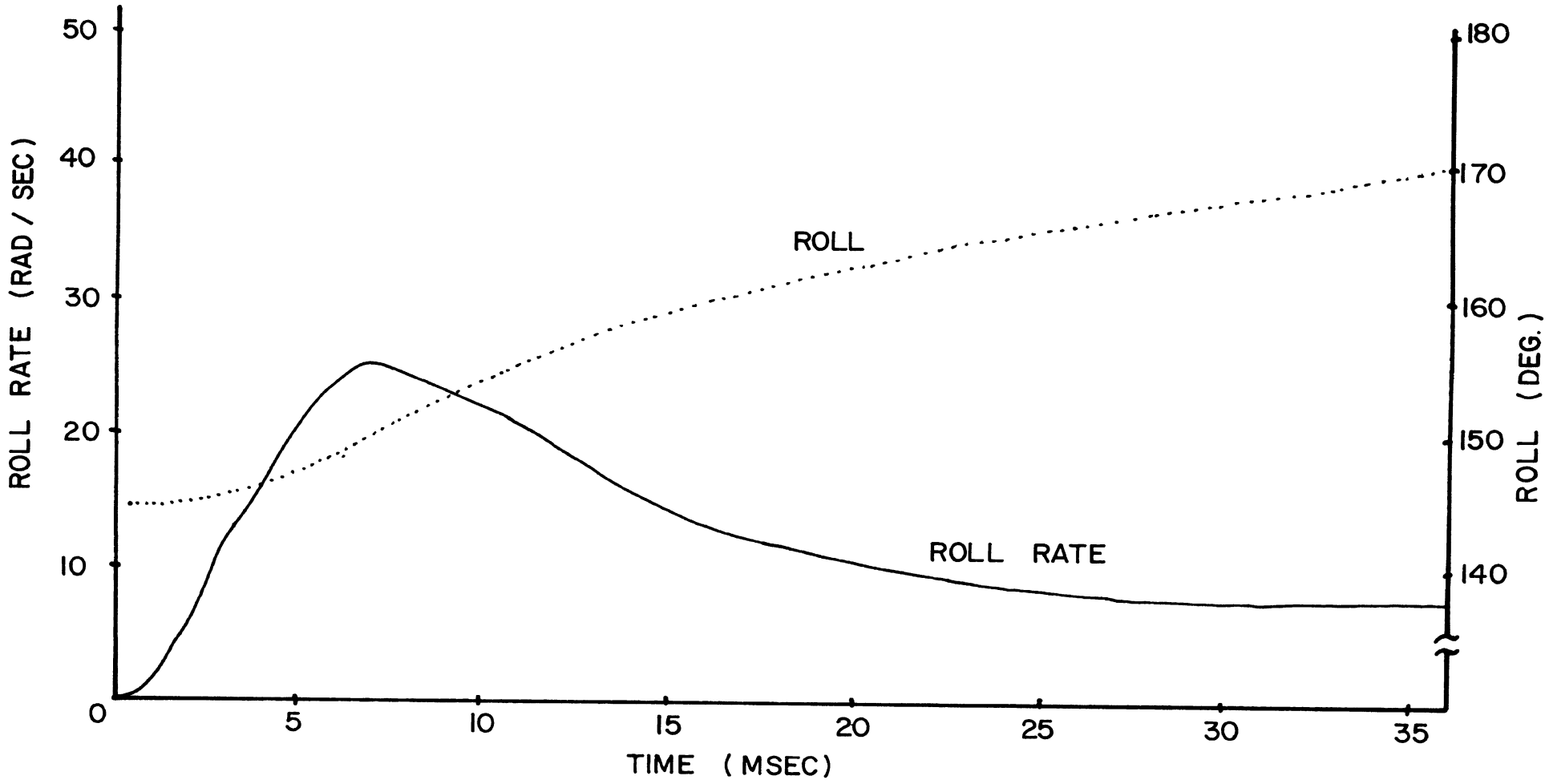

FIG.13

3.0 RESULTS

3.1 Task 1

Two cadavers were impacted in the head as described in Section 2.1.1. Of the two a complete data set was only obtained from VRIC-1. In the other case, loss of one or more accelerometer channels rendered the analysis impossible. Redundant accelerometers are now being used to insure analysis as well as acting as a check on the integration routine of the motion analysis.

The test set-up for VRIC-1 is shown in Figure 7. The results of this impact are presented in Figures 8-13. These curves represent the input force as well as the resultant head motion with respect to the axes described in 2.2.

The head severity index is also presented. There was no external damage to the cadaver's head and no skull fracture was observed at autopsy. The brain was examined externally as well as internally with only slight congestion observed. The overall injury level based on this information would be considered mild, but it should be pointed out that cadavers generally give lower injury levels than are observed in living humans.

More impacts are being carried out under the second year study of this program which is being sponsored by the Motor Vehicle Manufacturers Association.

3.2 Task 4

Five cadavers were impacted on the knees for a total of seven impacts under Task 5. The impact stroke, impactor surface, and impactor velocity were all varied in these first seven impacts. Surprisingly large forces without fracture were observed and this was the reason for varying these parameters. Fracture was finally obtained in one case.

The test set-up for a knee impact is shown in Figure 14. The results of the seven leg impacts are shown in Figures 15-19. The velocity of impact, leg impacted, available piston kinetic energy, and impactor stroke are all listed on the figures.

No injuries were observed by X-ray of any of the legs except VRIC-4. Figures 20 and 21 show x-rays of the fracture to the right leg of VRIC-4. The fracture load was recorded to be 4,400 lbs. A detailed examination of the legs will be conducted in the Fall of 1974, and reported in the MVMA final report.

A summary of all of the VRIC cadaver tests is shown in Table 1 and the anthropometry data is given for all cadavers in Appendix C. Tasks 2, 3, and 5 are being conducted under the new sponsorship of MVMA with the final report due in June 1975.

4.0 CONCLUSIONS

The purpose of the first year of this project was to set up the experimental procedures to carry out Tasks 1 through 5 as given in Section 1. All of the test procedures were developed during this phase of the study.

Some preliminary experiments were run at the end of the project to check out the systems and procedures for the individual tasks. The results of these tests indicate that head motion can be determined from accelerometers mounted to the head, and that some injuries to the brain can be observed.

Considerably higher forces than have been previously published were observed with no leg fracture of any kind. The exact mechanisms as well as impact conditions for leg fracture have not been determined. Additional experiments have been added to this study to allow for further examination of the conditions and mechanisms for fracture. These additions will be carried out under the MVMA study.

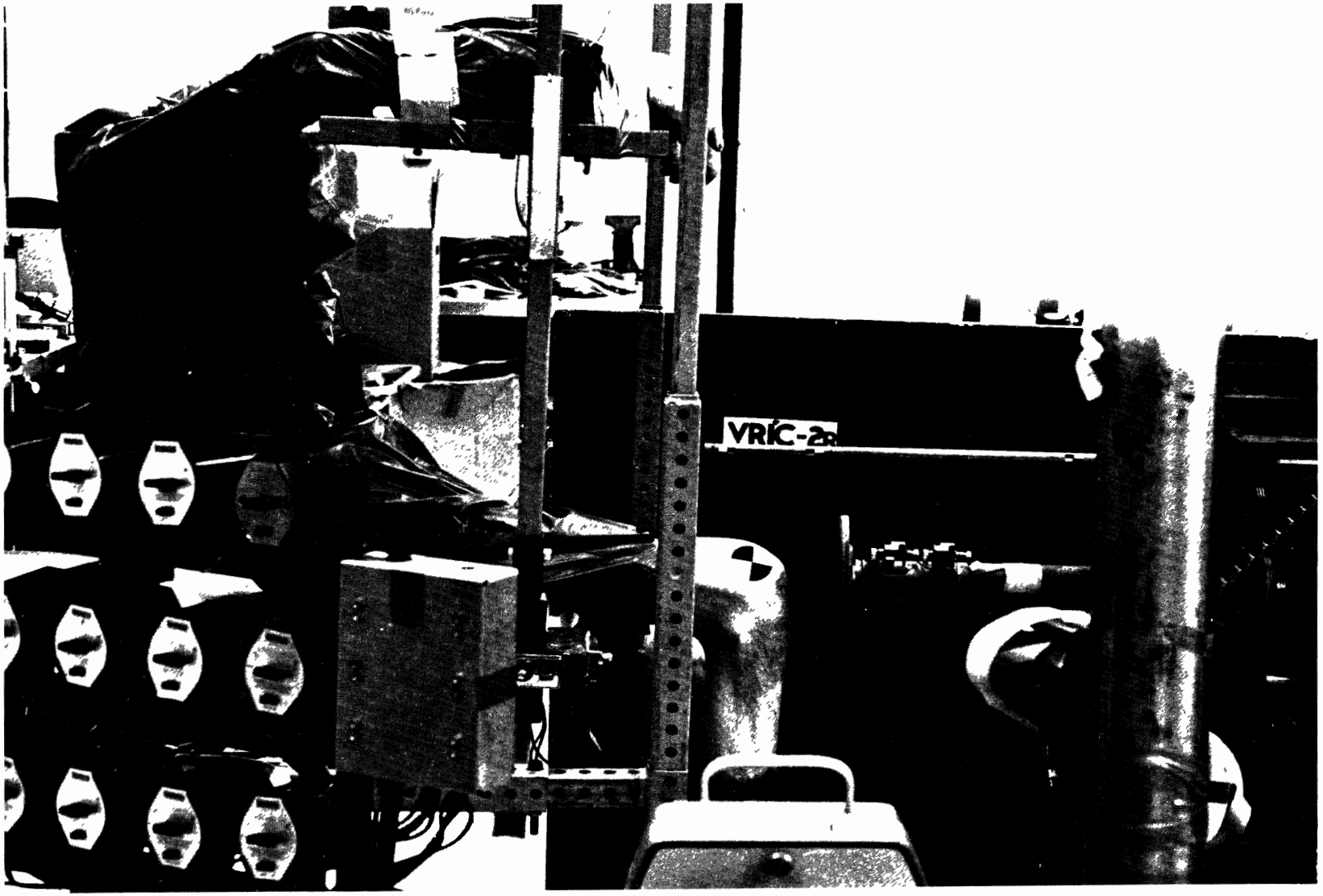

FIGURE 14. TEST SET-UP FOR KNEE IMPACTS

FIG. 15 : LEG IMPACT FOR VRIC-1

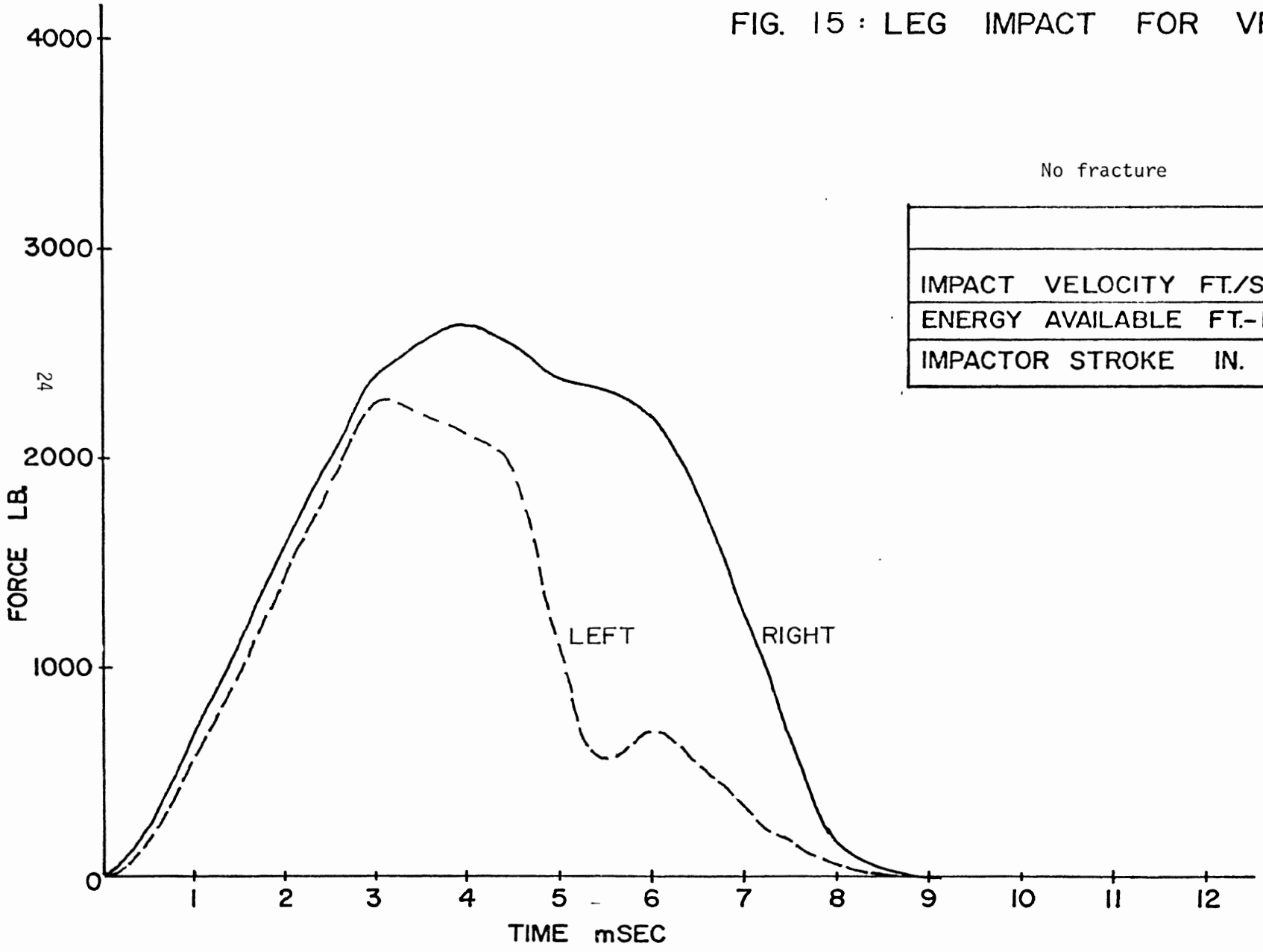

No fracture

	RIGHT	LEFT
IMPACT VELOCITY FT./SEC.	2330	2262
ENERGY AVAILABLE FT.-LB.	388	365
IMPACTOR STROKE IN.	2.5	2.5

FIG. 16 : LEG IMPACT FOR VRIC-2

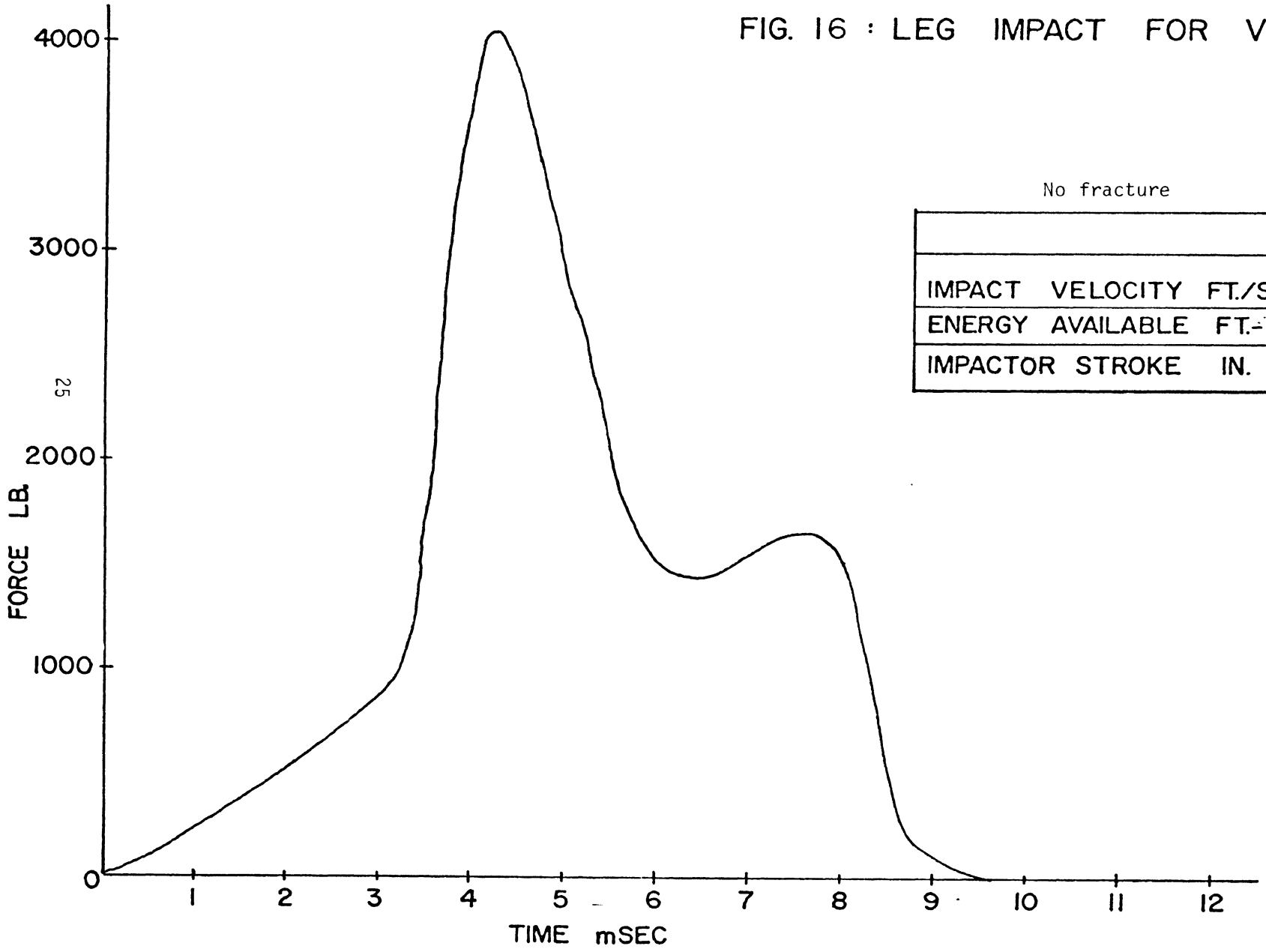

No fracture

	RIGHT	LEFT
IMPACT VELOCITY FT./SEC.		20.70
ENERGY AVAILABLE FT.-LB.		306
IMPACTOR STROKE IN.		2.5

FIG. 17 : LEG IMPACT FOR VRIC-3

No fracture

	RIGHT	LEFT
IMPACT VELOCITY FT./SEC.	35.84	21.96
ENERGY AVAILABLE FT.-LB.	917	344
IMPACTOR STROKE IN.	2.5	2.5

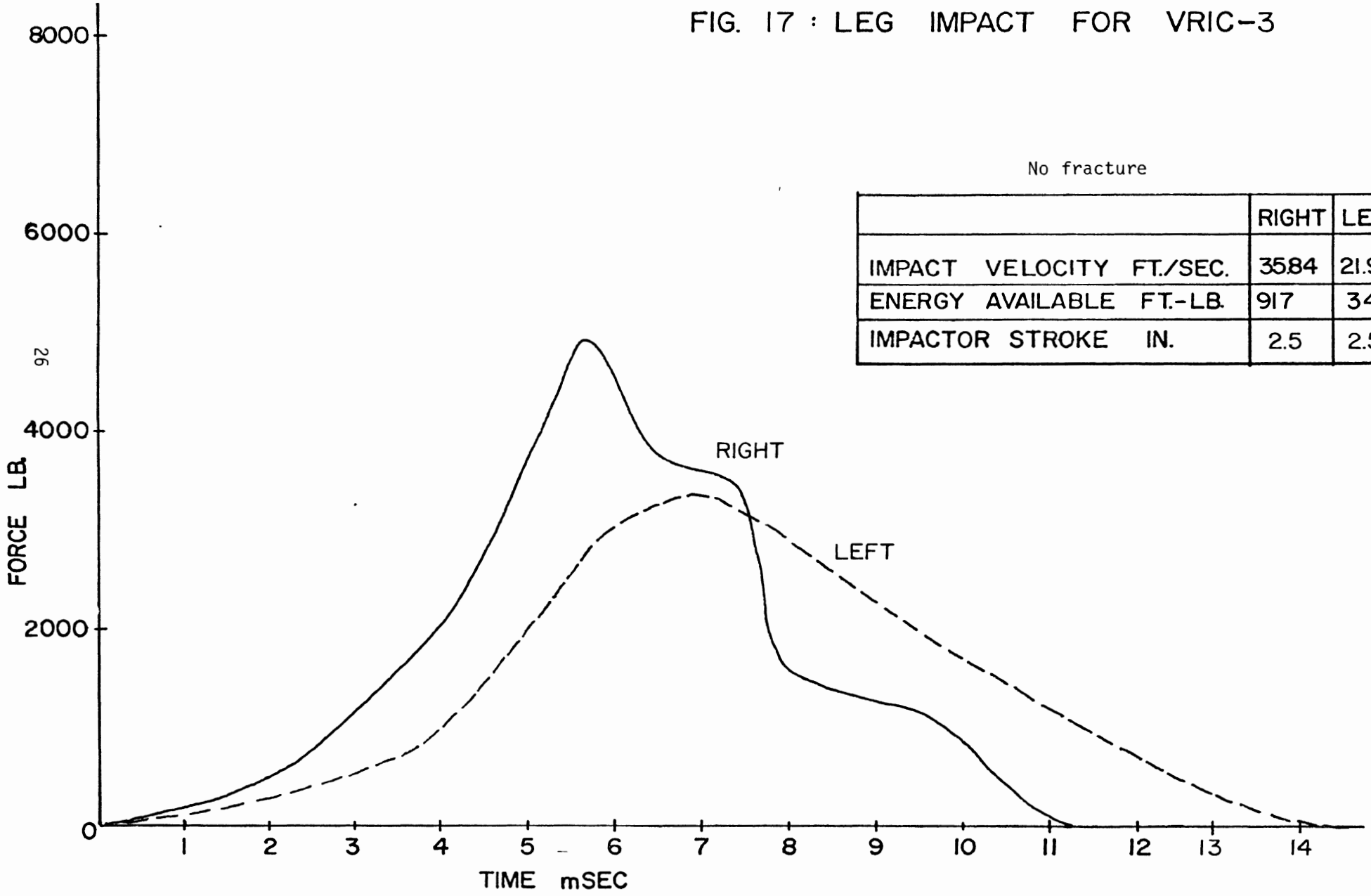

FIG. 18 : LEG IMPACT FOR VRIC-4

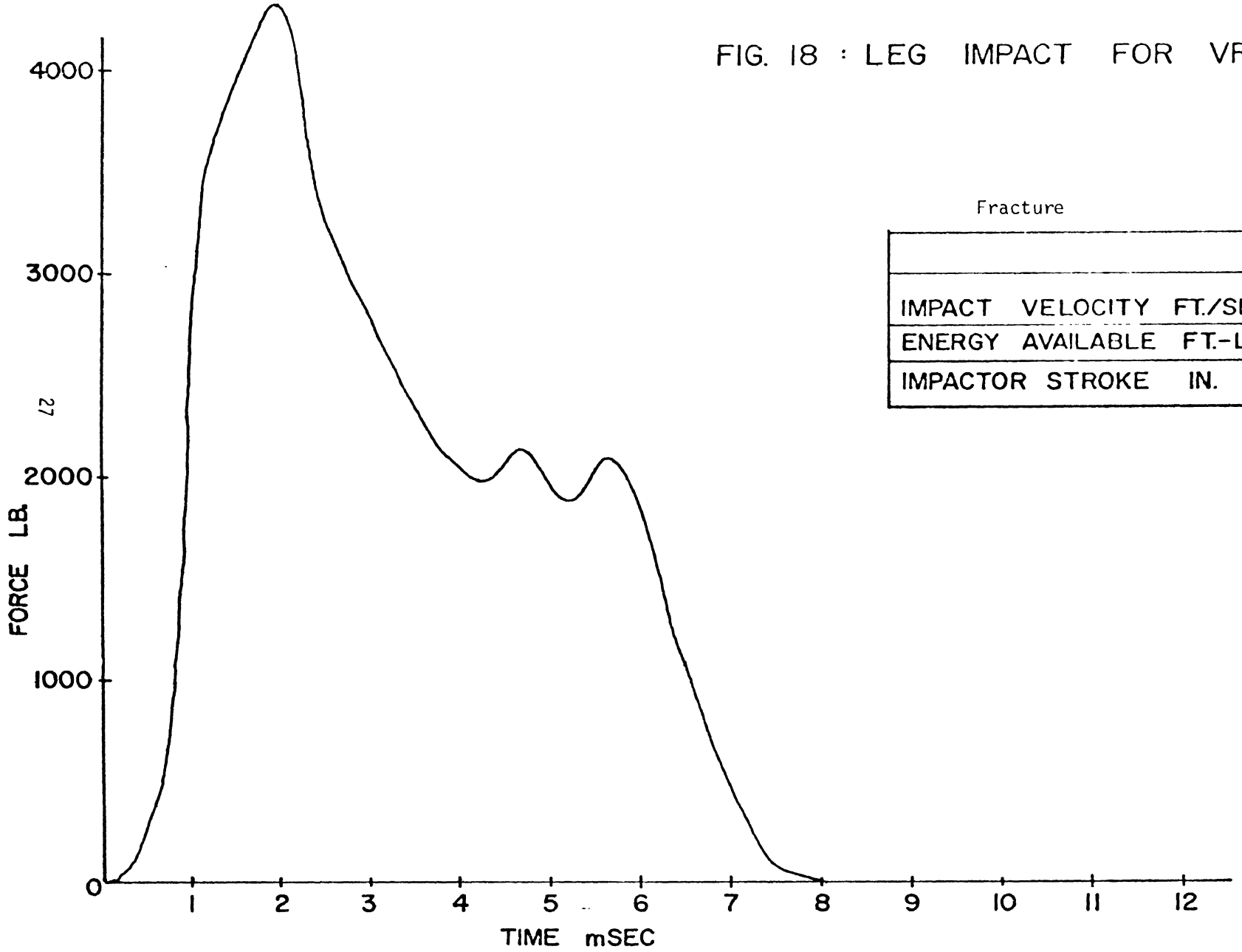

Fracture

	RIGHT	LEFT
IMPACT VELOCITY FT./SEC.	38.06	
ENERGY AVAILABLE FT.-LB.	1034	
IMPACTOR STROKE IN.	4.25	

FIG. 19 : LEG IMPACT FOR VRIC-5

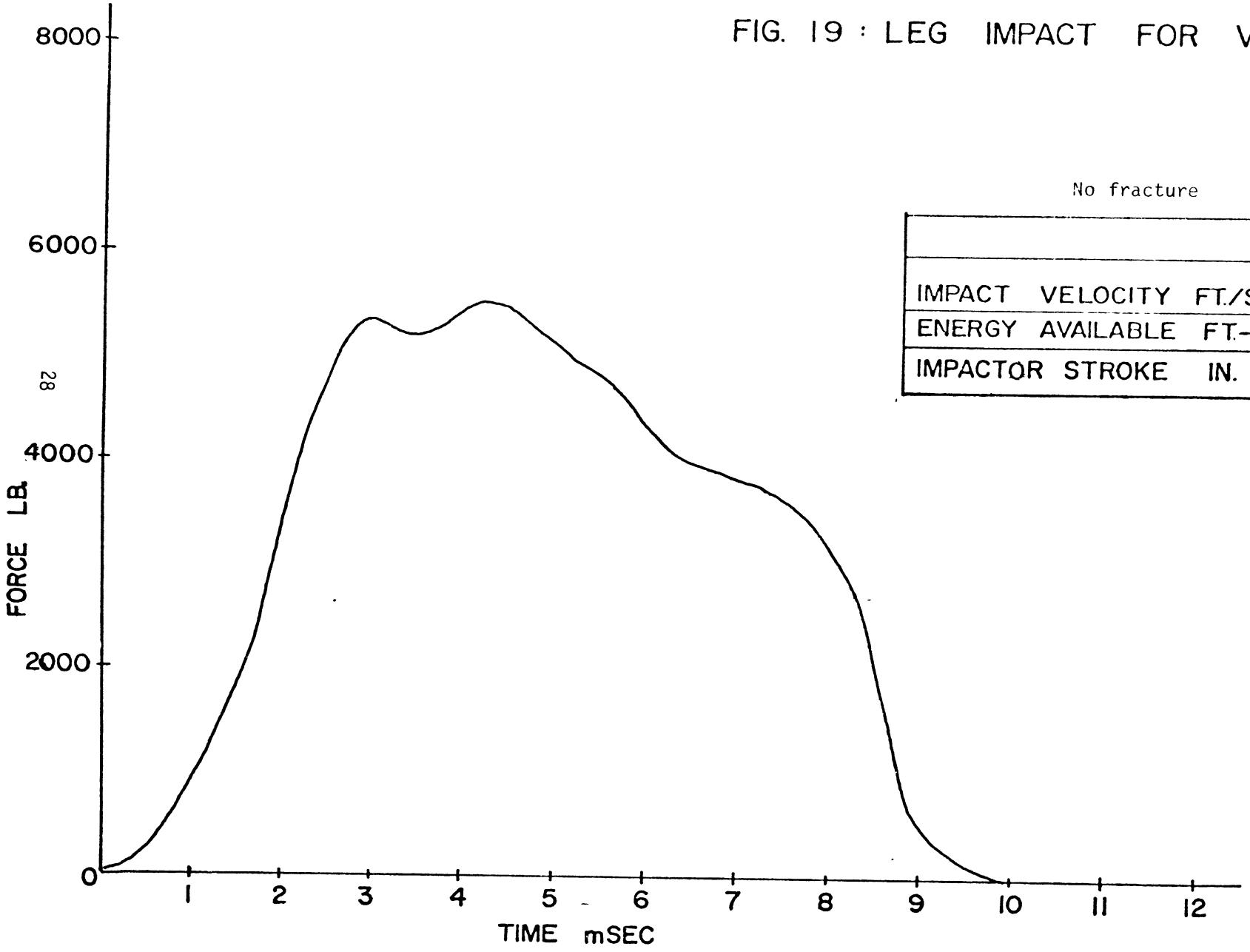

No fracture

	RIGHT	LEFT
IMPACT VELOCITY FT./SEC.	34.18	
ENERGY AVAILABLE FT.-LB.	834	
IMPACTOR STROKE IN.	2.25	

FIGURE 20. L-R X-RAY OF VRIC-4 LEG FRACTURE

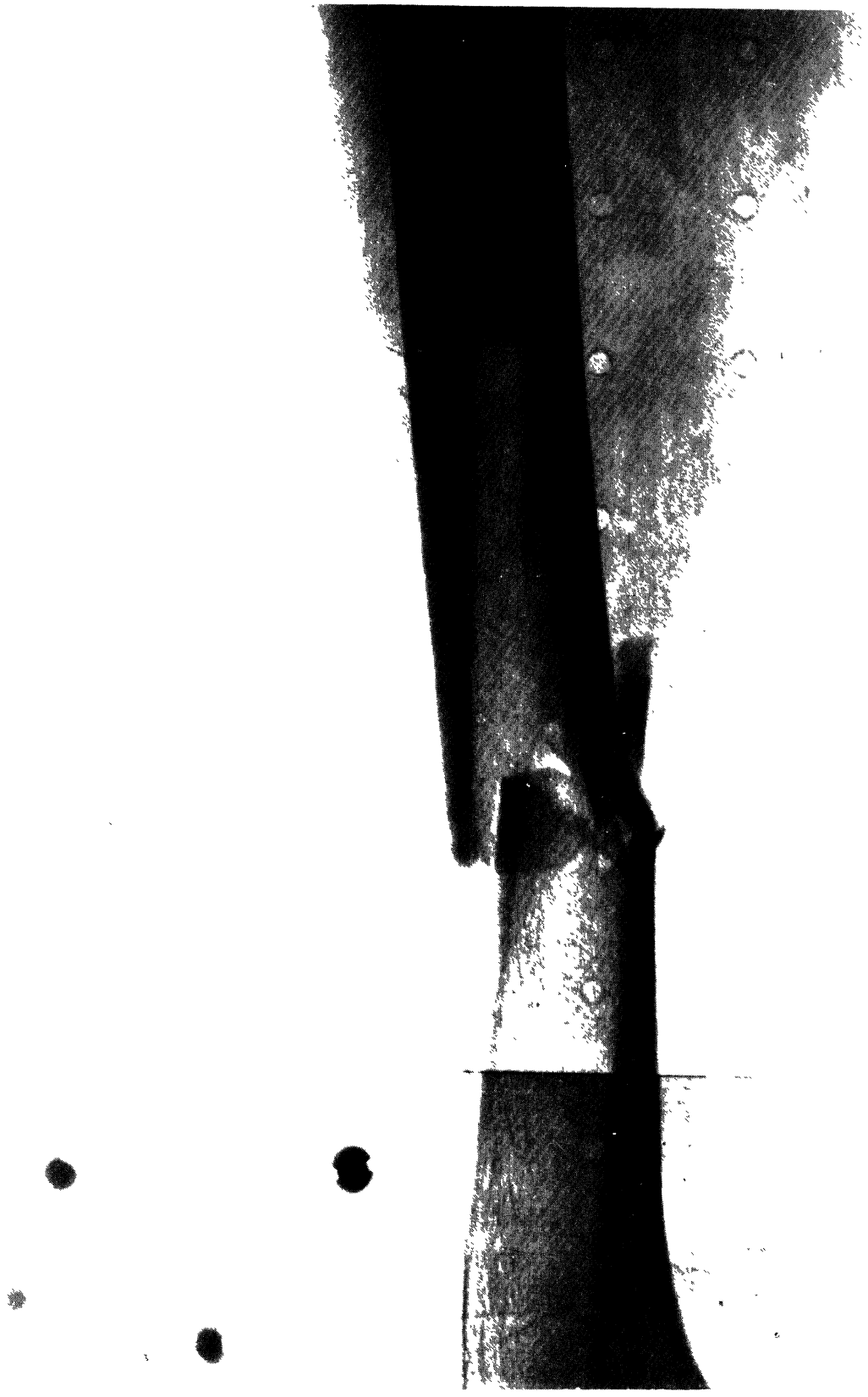

FIGURE 21. A-P X-RAY OF VRIC-4 LEG FRACTURE

TABLE 1

VRIC SUMMARY SHEET

Test No.	Height ft-in	Weight lb	Age Yrs	Sex	Cause of Death	Head Impact Data: Impact Vel. ft/sec	Impact Force lb	Force Duration msec	Peak Linear Resul. Accel. G's	Peak Ang. Resul. Accel. k rad/sec²	Severity Index	Knee Impact Data: Leg	Impact Vel. ft/sec	Impact Force lb	Force Duration msec	Impact Energy ft-lb	Stroke in	Comments and Injury
VRIC-1	5-6	149	90	M	Acute Pulmonary Edema, Hypertension Arteriolosclerosis	22.1	2250	10	180	17.3	1100	L	22.62	2300	8.5	365	2.5	Brain congestion. No leg fracture.
												R	23.30	2700	9.0	388	2.5	
VRIC-2	-	133	57	M	Bronchial Pneumonia, Cardiovascular arrest.	-	-	-	-	-	-	L	20.7	4000	9.5	306	2.5	No fracture.
												R	-	-	-	-	-	
VRIC-3	5-9.5	178	51	M	-	21.8	3200	12	LOD	LOD	LOD	L	21.9	3500	14	344	2.5	Brain congestion. No leg fracture.
												R	35.8	-	11	917	2.5	
VRIC-4	-	128	83	F	Cerebral Thrombosis	-	-	-	-	-	-	L	-	-	-	-	-	Fracture
												R	38.1	4400	8	1034	4.25	
VRIC-5	-	184	77	M	Cerebral Vascular Accident	-	-	-	-	-	-	L	-	-	-	-	-	No fracture.
												R	34.2	5500	10	834	2.25	

L.O.D. = Loss of Data

\- = Not tested

REFERENCE

1. Ewing, Channing L. and Thomas, Daniel J., "Human Head and Neck Response to Impact Acceleration," NAMRL Monograph 21, Naval Aerospace Medical Research Laboratory, U.S. Army Aeromedical Research Laboratory, 1972.

APPENDIX A

HEAD MOTION DETERMINATION

APPENDIX A HEAD MOTION DETERMINATION

A.1 Introduction

The experimental determination of the three-dimensional rigid body motion of the head required the development of three basic techniques:

1. An appropriate theoretical analysis technique to calculate the overall motion based on accelerometer information.
2. An appropriate method for installing and locating the accelerometers on the head.
3. An appropriate radiographic technique for locating the accelerometers with respect to anatomical landmarks.

These three techniques are detailed in the following sections of this appendix.

A.2 Theoretical Analysis of Head Motion

A number of accelerometers attached to a rigid body can provide enough information to completely determine its motion with respect to an inertial reference frame providing the following conditions are met:

(1) A minimum of 6 accelerometers are used.

(2) They are distributed over at least 3 different non-collinear locations.

(3) Their respective directions must be such that the axes of at least one pair of accelerometers be parallel to the axes of an arbitrarily chosen orthogonal coordinate system on that body. (An orthogonal coordinate system is chosen for convenience only.)

For the minimum 3 locations, Q_1, Q_2, Q_3 on a rigid body, nine scalar equations can be used to describe the motion of the rigid body with respect to an inertial frame.

For the rigid body shown in Figure A1.

FIGURE A1

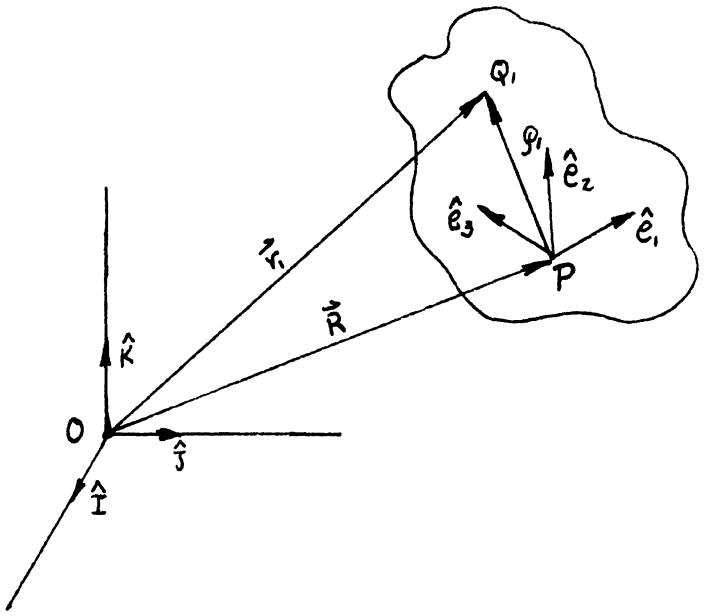

where $O(\hat{I}\ \hat{J}\ \hat{K})$: inertial point and frame

$P(\hat{e}_1, \hat{e}_2, \hat{e}_3)$: particular point and moving frame on the rigid body

Q : general point on the rigid body

$\vec{\omega}$: absolute average velocity of rigid body (relative to inertial)

$\dot{\vec{\omega}}$: absolute average acceleration of rigid body

$\vec{OP} = \vec{R}$: vector position point P (absolute)

$\vec{PQ_1} = \vec{\rho}$: position of Q relative to (e_1, e_2, e_3)

$\vec{OQ_1} = \vec{r}_1$: position of Q, absolute

$$\ddot{\vec{R}} = g_1 \hat{e}_1 + g_2 \hat{e}_2 + g_3 \hat{e}_3 \qquad \vec{\omega} = \omega_1 \hat{e}_1 + \omega_2 \hat{e}_2 + \omega_3 \hat{e}_3$$

$$\ddot{\vec{\rho}} = b_{11} \hat{e}_1 + b_{21} \hat{e}_2 + b_{31} \hat{e}_3 \qquad \dot{\vec{\omega}} = \alpha_1 \hat{e}_1 + \alpha_2 \hat{e}_2 + \alpha_3 \hat{e}_3$$

The nine scalar equations for points Q_1, Q_2, Q_3 are:

For P & Q_1:

Set I
$$\begin{cases} (g_1 - b_{11}) + (\alpha_2 \rho_{31} - \alpha_3 \rho_{21}) + \omega_1(\omega_2 \rho_{21} + \omega_3 \rho_{31}) - \rho_{11}(\omega_2^2 + \omega_3^2) = 0 \\ (g_2 - b_{21}) + (\alpha_3 \rho_{11} - \alpha_1 \rho_{31}) + \omega_2(\omega_1 \rho_{11} + \omega_3 \rho_{31}) - \rho_{21}(\omega_1^2 + \omega_3^2) = 0 \\ (g_3 - b_{31}) + (\alpha_1 \rho_{21} - \alpha_2 \rho_{11}) + \omega_3(\omega_1 \rho_{11} + \omega_2 \rho_{21}) - \rho_{31}(\omega_1^2 + \omega_2^2) = 0 \end{cases}$$

For P & Q_2:

$$\text{Set II}\begin{cases}(g_1-b_{12})+(\alpha_2\rho_{32}-\alpha_3\rho_{22})+\omega_1(\omega_2\rho_{22}+\omega_3\rho_{32})-\rho_{12}(\omega_2^2+\omega_3^2)=0\\(g_2-b_{22})+(\alpha_3\rho_{12}-\alpha_1\rho_{32})+\omega_2(\omega_1\rho_{12}+\omega_3\rho_{32})-\rho_{22}(\omega_1^2+\omega_3^2)=0\\(g_3-b_{32})+(\alpha_1\rho_{22}-\alpha_2\rho_{12})+\omega_3(\omega_1\rho_{12}+\omega_2\rho_{22})-\rho_{32}(\omega_1^2+\omega_2^2)=0\end{cases}$$

And for P & Q_3:

$$\text{Set III}\begin{cases}(g_1-b_{13})+(\alpha_2\rho_{33}-\alpha_3\rho_{23})+\omega_1(\omega_2\rho_{23}+\omega_3\rho_{33})-\rho_{13}(\omega_2^2+\omega_3^2)=0\\(g_2-b_{23})+(\alpha_3\rho_{13}-\alpha_1\rho_{33})+\omega_2(\omega_1\rho_{13}+\omega_3\rho_{33})-\rho_{23}(\omega_1^2+\omega_3^2)=0\\(g_3-b_{33})+(\alpha_1\rho_{23}-\alpha_2\rho_{13})+\omega_2(\omega_1\rho_{13}+\omega_2\rho_{23})-\rho_{33}(\omega_1^2+\omega_2^2)=0\end{cases}$$

The 6 accelerometers may be distributed over 3 points in either of 2 combinations:

	Q_1	Q_2	Q_3
Combination A	3	2	1
Combination B	2	2	2

Depending upon the particular combination and accelerometer orientation used (in accordance to the aforementioned rules), 6 of the 9 values, b_{11}, b_{21}, b_{31}, b_{12}, b_{22}, b_{32}, b_{13}, b_{23}, b_{33}, will be known, as well as the components of $\vec{\rho}_1$, $\vec{\rho}_2$, $\vec{\rho}_3$.

After some manipulations, 3 of the 9 equations above can be used to find $\alpha_{1,2,3}$ and $\omega_{1,2,3}$. Part B describes this process in further detail for Combination B (2-2-2).

Then, Euler Angles θ, ψ, ϕ can be defined at point P giving the following relation.

$$\begin{Bmatrix} \dot{\theta} \\ \dot{\psi} \\ \dot{\phi} \end{Bmatrix} = [\Lambda]^{-1} \begin{Bmatrix} \omega_1 \\ \omega_2 \\ \omega_3 \end{Bmatrix}$$

where

$$[\Lambda] = \begin{bmatrix} \cos\phi & \sin\theta\sin\phi & 0 \\ \sin\phi & -\sin\theta\cos\phi & 0 \\ 0 & \cos\theta & 1 \end{bmatrix}$$

Numerical integration of this set of equations would give θ, ψ, & ϕ, the Euler angles for the rigid body.

Next, by using θ, ψ, and ϕ the Euler Transformation from $\hat{e}_1$ $\hat{e}_2$ $\hat{e}_3$ to $\hat{\mathbf{I}}$ $\hat{\mathbf{J}}$ $\hat{\mathbf{K}}$ can be calculated. Then, using this transformation, expressions for $\ddot{x}$, $\ddot{y}$, $\ddot{z}$ can be written for any point on the rigid body in terms of the known acceleration components at that point relative to $\hat{e}_1$ $\hat{e}_2$ $\hat{e}_3$.

In particular, for point P,

$$\ddot{x} = g_1(\cos\psi\cos\phi - \cos\theta\sin\phi\sin\psi) + g_2(-\sin\psi\cos\phi - \sin\theta\sin\phi\cos\psi) + g_3(\sin\theta\cos\phi)$$

$$\ddot{y} = g_1(\cos\psi\sin\phi + \cos\theta\cos\phi\sin\psi) + g_2(-\sin\psi\sin\phi + \cos\theta\cos\phi\cos\psi) + g_3(-\sin\theta\cos\phi)$$

$$\ddot{z} = g_1(\sin\psi\sin\theta) + g_2(\cos\psi\sin\theta) + g_3(\cos\theta)$$

Two single numerical integrations of these equations will then give linear absolute velocities and accelerations as well as the x, y, z, absolute positon of that point.

Hence, the orientation of the head (treated as a rigid body), its angular velocity and angular acceleration, and the linear absolute velocities and accelerations of the 3 points on the head may be determined from a minimum of 6 accelerometers located on the head.

B- 2-2-2 Combination

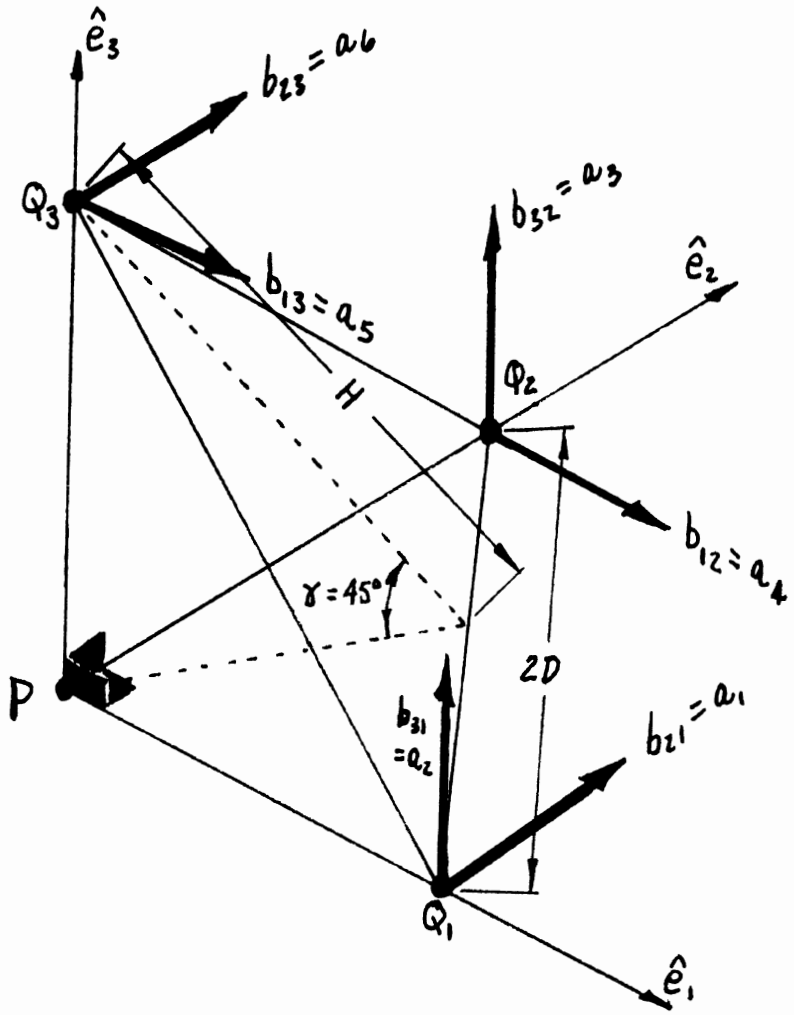

Figure A-2. 2-2-2 Combination

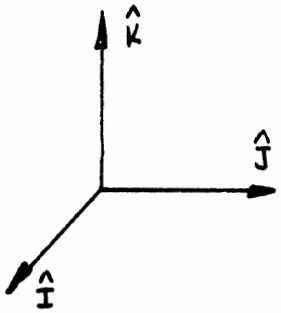

For this arrangement,

$$\left.\begin{aligned}\vec{PQ}_1 &= \rho_{11}\hat{e}_1 + \rho_{21}\hat{e}_2 + \rho_{31}\hat{e}_3\\ \vec{PQ}_2 &= \rho_{12}\hat{e}_1 + \rho_{22}\hat{e}_2 + \rho_{32}\hat{e}_3\\ \vec{PQ}_3 &= \rho_{13}\hat{e}_1 + \rho_{23}\hat{e}_2 + \rho_{33}\hat{e}_3\end{aligned}\right\} \text{ reduce to } \left\{\begin{aligned}\vec{PQ}_1 &= \rho_{11}\hat{e}_1\\ \vec{PQ}_2 &= \rho_{22}\hat{e}_2\\ \vec{PQ}_3 &= \rho_{33}\hat{e}_3\end{aligned}\right.$$

and for $\gamma = 45°$,

$$\rho_{11} = \sqrt{D^2 + H^2/2}$$
$$\rho_{22} = \sqrt{D^2 + H^2/2}$$
$$\rho_{33} = \sqrt{H^2/2}$$

Dropping terms not containing ρ_{11}, ρ_{22}, ρ_{33} in the original 9 scalar equations relative to point P and subtracting the resulting equations (by sets) in the manner (II,I), III-II), & (I-II) gives nine equations which do not contain g_1, g_2, g_3;

$(\text{II}-\text{I})$:

$$\text{I}'\begin{cases}(b_{11}-b_{12})+\rho_{22}(\omega_1\omega_2-\dot{\omega}_3)+\rho_{11}(\omega_2^2+\omega_3^2)=0\\(b_{21}-b_{22})-\rho_{22}(\omega_1^2+\omega_3^2)-\rho_{11}(\omega_2\omega_1+\dot{\omega}_3)=0\\(b_{31}-b_{32})+\rho_{22}(\omega_3\omega_2+\dot{\omega}_1)-\rho_{11}(\omega_3\omega_1-\dot{\omega}_2)=0\end{cases}\quad *$$

$(\text{III}-\text{II})$:

$$\text{II}'\begin{cases}(b_{12}-b_{13})+\rho_{33}(\omega_1\omega_3+\dot{\omega}_2)-\rho_{22}(\omega_1\omega_2-\dot{\omega}_3)=0\\(b_{22}-b_{23})+\rho_{33}(\omega_2\omega_3-\dot{\omega}_1)+\rho_{22}(\omega_1^2+\omega_3^2)=0\\(b_{32}-b_{33})-\rho_{33}(\omega_1^2+\omega_2^2)-\rho_{22}(\omega_3\omega_2+\dot{\omega}_1)=0\end{cases}\quad *$$

$(\text{I}-\text{III})$:

$$\text{III}'\begin{cases}(b_{13}-b_{11})-\rho_{11}(\omega_2^2+\omega_3^2)-\rho_{33}(\omega_1\omega_3+\dot{\omega}_2)=0\\(b_{23}-b_{21})+\rho_{11}(\omega_2\omega_1+\dot{\omega}_3)-\rho_{33}(\omega_2\omega_3-\dot{\omega}_1)=0\\(b_{33}-b_{31})+\rho_{11}(\omega_3\omega_1-\dot{\omega}_2)+\rho_{33}(\omega_1^2+\omega_2^2)=0\end{cases}\quad *$$

Selecting the 3 starred equations which can be solved for α_1 α_2 and α_3 from the 6 accelerometer readings gives after rearrangement:

(1) $\dot{\omega}_1\rho_{22}+\dot{\omega}_2\rho_{11}=(b_{32}-b_{31})+\omega_3(\omega_1\rho_{11}-\omega_2\rho_{22})$

(2) $\dot{\omega}_2\rho_{33}+\dot{\omega}_3\rho_{22}=(b_{13}-b_{12})+\omega_1(\omega_2\rho_{22}-\omega_3\rho_{33})$

(3) $\dot{\omega}_3\rho_{11}+\dot{\omega}_1\rho_{33}=(b_{21}-b_{23})+\omega_2(\omega_3\rho_{33}-\omega_1\rho_{11})$

And using the substitutions,

$\rho_{11}=d_1$	$b_{21}=a_1$	$b_{31}=a_2$
$\rho_{22}=d_2$	$b_{32}=a_3$	$b_{12}=a_4$
$\rho_{33}=d_3$	$b_{13}=a_5$	$b_{23}=a_6$

these 3 equations become:

(1) $$\dot{\omega}_1=\dot{\alpha}_1=\frac{-(a_5-a_4)d_1+(a_1-a_6)d_2+(a_3-a_2)d_3}{2d_2d_3}-\frac{\omega_1d_1(\omega_2d_2-\omega_3d_3)}{d_2d_3}$$

$$\textcircled{2}\quad \dot{\omega}_2 = \alpha_2 = \frac{(a_5-a_4)d_1-(a_1-a_6)d_2+(a_3-a_2)d_3}{2d_1d_3} - \frac{\omega_2 d_2(\omega_3 d_3-\omega_1 d_1)}{d_1 d_3}$$

$$\textcircled{3}\quad \dot{\omega}_3 = \alpha_3 = \frac{(a_5-a_4)d_1+(a_1-a_6)d_2-(a_3-a_2)d_3}{2d_1d_2} - \frac{\omega_3 d_3(\omega_1 d_1-\omega_2 d_2)}{d_1 d_3}$$

These, then, can be numerically integrated given the values

Initial Conditions	Geometry	Acceleration Values
$\omega_1(0)$	d_1	(a_5-a_4)
$\omega_2(0)$	d_2	(a_1-a_6)
$\omega_3(0)$	d_3	(a_3-a_2)

to give ω_1, ω_2 & ω_3.

Next, the absolute acceleration components, g_1, g_2, g_3 transformation can be calculated from known quantities.

$$g_1 = \tfrac{1}{2}\left[a_4+a_5+d_2(\omega_3^2+\omega_1^2)+d_3(\omega_1^2+\omega_2^2)\right]$$

$$g_2 = \tfrac{1}{2}\left[a_1+a_6-d_1(\alpha_3+\omega_3\omega_1)-d_3(\alpha_2+\omega_1\omega_3)\right]$$

$$g_3 = \tfrac{1}{2}\left[a_2+a_3-d_1(\omega_3\omega_1-\alpha_2)-d_2(\omega_3\omega_2-\alpha_3)\right]$$

and x, y, z can be determined.

A.3. Accelerometer Installation Fixture

An installation fixture is required for accurate placement of the head accelerometers. This fixture should meet the following conditions:

1. Be adjustable to different head sizes.

2. Be insensitive to skull irregularities.

3. Be capable of mounting accelerometers in an unsymmetrical pattern on head to allow clearance for impact device.

4. Ensure that accelerometers are mounted in an orthogonal relationship as depicted in Figure A-3.

5. Allow position vectors ρ_1, ρ_2 and ρ_3, the distance from the instrumentation coordinate system origin to the respective accelerometer pairs, to be obtained. (See Figure A-3).

6. Accelerometers should remain rigidly attached to head in the correct orientation when fixture is removed.

The HSRI accelerometer installation fixture, shown in Figure A-4, consists of a base and three arms whose upper edge surfaces are parallel to the theoretical instrumentation coordinate system. A sliding block on each arm provides the adjustment for different head sizes ahd various accelerometer groupings, and each block locks into position with a single bolt.

The actual attachment to the head is by means of three flanged collet and threaded cup assemblies. Each assembly clamps from both sides of the skull through a 6 mm drilled hole and provides a very rigid platform upon which to mount accelerometers. An accelerometer mount is potted in position in the open face of each cup, and two Wilcoxon Research accelerometers thread into each mount in a biaxial configuration. A drawing of a typical installed assembly is shown in Figure A-5. The correct alignment of the accelerometer mounts is provided by the sliding blocks on the fixture, which hold the

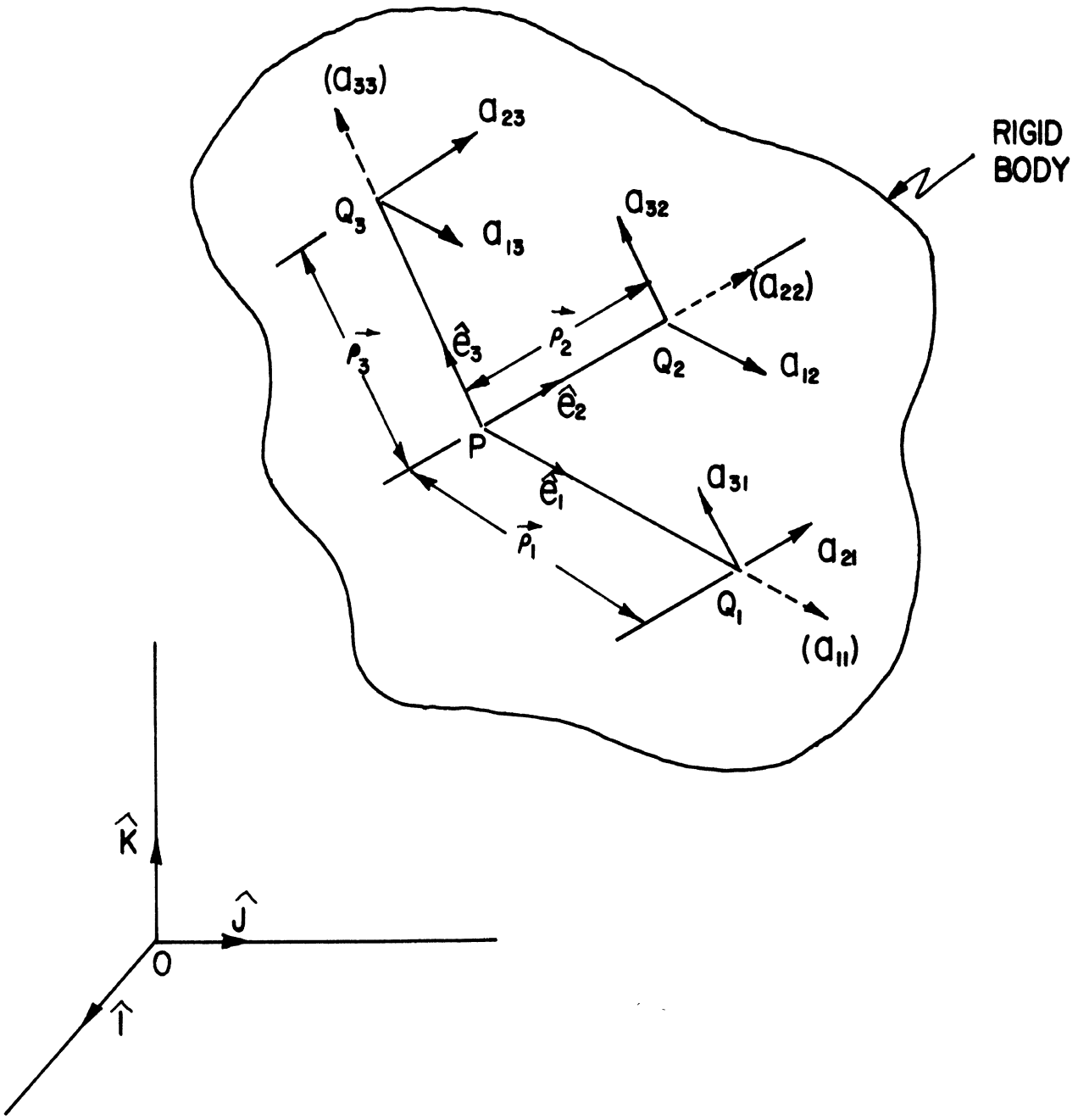

$(\hat{I},\hat{J},\hat{K})$: INERTIAL COORDINATE SYSTEM, ORIGIN O

$(\hat{e}_1,\hat{e}_2,\hat{e}_3)$: INSTRUMENTATION COORD. SYST., ORIGIN P

(Q_1,Q_2,Q_3): CENTER OF MASSES OF 3 PAIRS OF ACCELEROMETERS

FIGURE A3: INSTRUMENTATION COORDINATE SYSTEM AND ACCELEROMETER ORIENTATION.

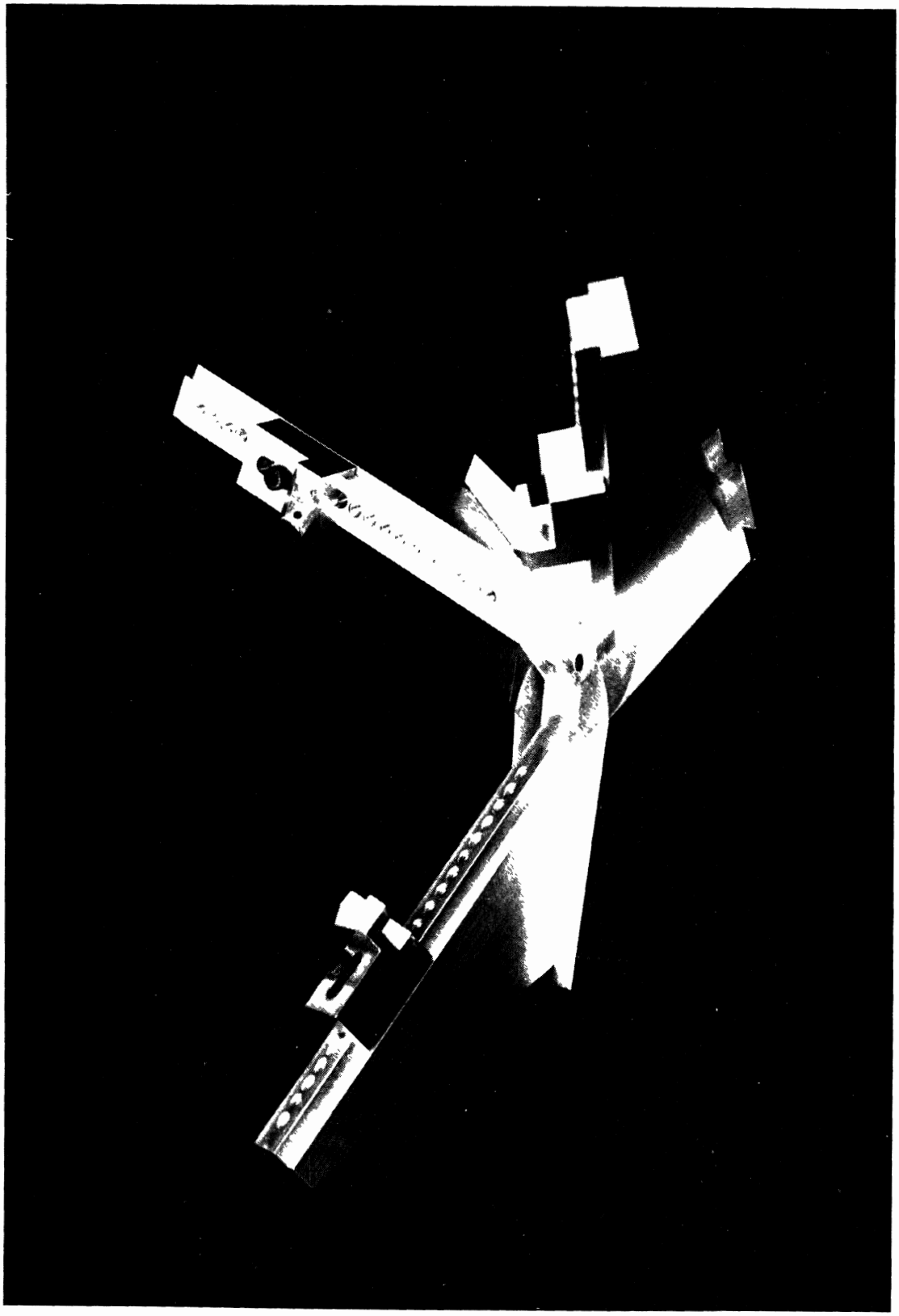

Figure A-4 Accelerometer Installation Fixture

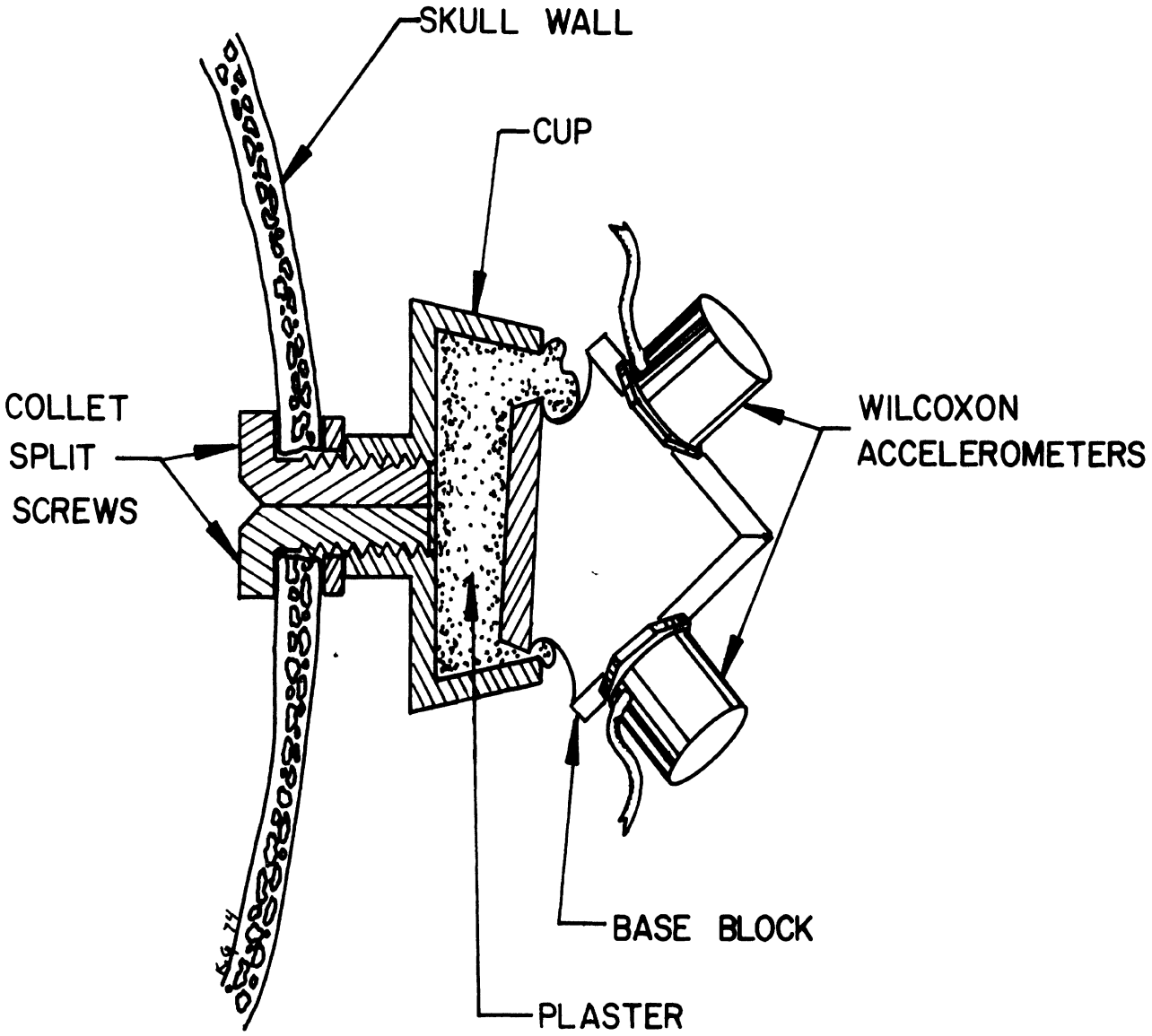

FIGURE A-5: COLLET, CUP, AND ACCELEROMETER ASSEMBLY

mounts in the desired orthogonal relationship while the potting material hardens. This use of potting technique allows a very high degree of precision in accelerometer placement since the alignment of the accelerometer mounts becomes dependent only on the machining tolerances of the installation fixture. The fixture and accelerometer mount assembly floats with respect to the cup and collet assemblies, and potting the accelerometer mount into the cup permits considerable angular misalignment of the cups from skull irregularities. Before the fixture is removed from the head, the distances from the end of each fixture arm to the end of its sliding block are measured (See Figure A-6) and these dimensions are used to calculate the position vectors ρ_1, ρ_2 and ρ_3 from the known geometry of the fixture.

The installation procedure is as follows:

1. Install accelerometer mounts into sliding blocks. Thread a tapered pointer into base of each mount. The tips of the pointers approximate the positions of the cup bases and are used to locate the holes in the skull.

2. Adjust the sliding blocks along the arms of the fixture until the pointers are at the most favorable position on the head for mounting the accelerometers. Lock the sliding blocks in this position. Mark the scalp where the pointers touch.

3. Cut a core of at least 3/8" diameter from the scalp concentric with each marked point.

4. Using the fixture, place the pointers against the skull and mark the points again. Reposition the sliding blocks if necessary to center the pointers within the cored hole in the scalp.

5. Label the fixture arms Q_1, Q_2, and Q_3 according to the convention shown in Figure A-3.

6. Drill the three holes in the skull.

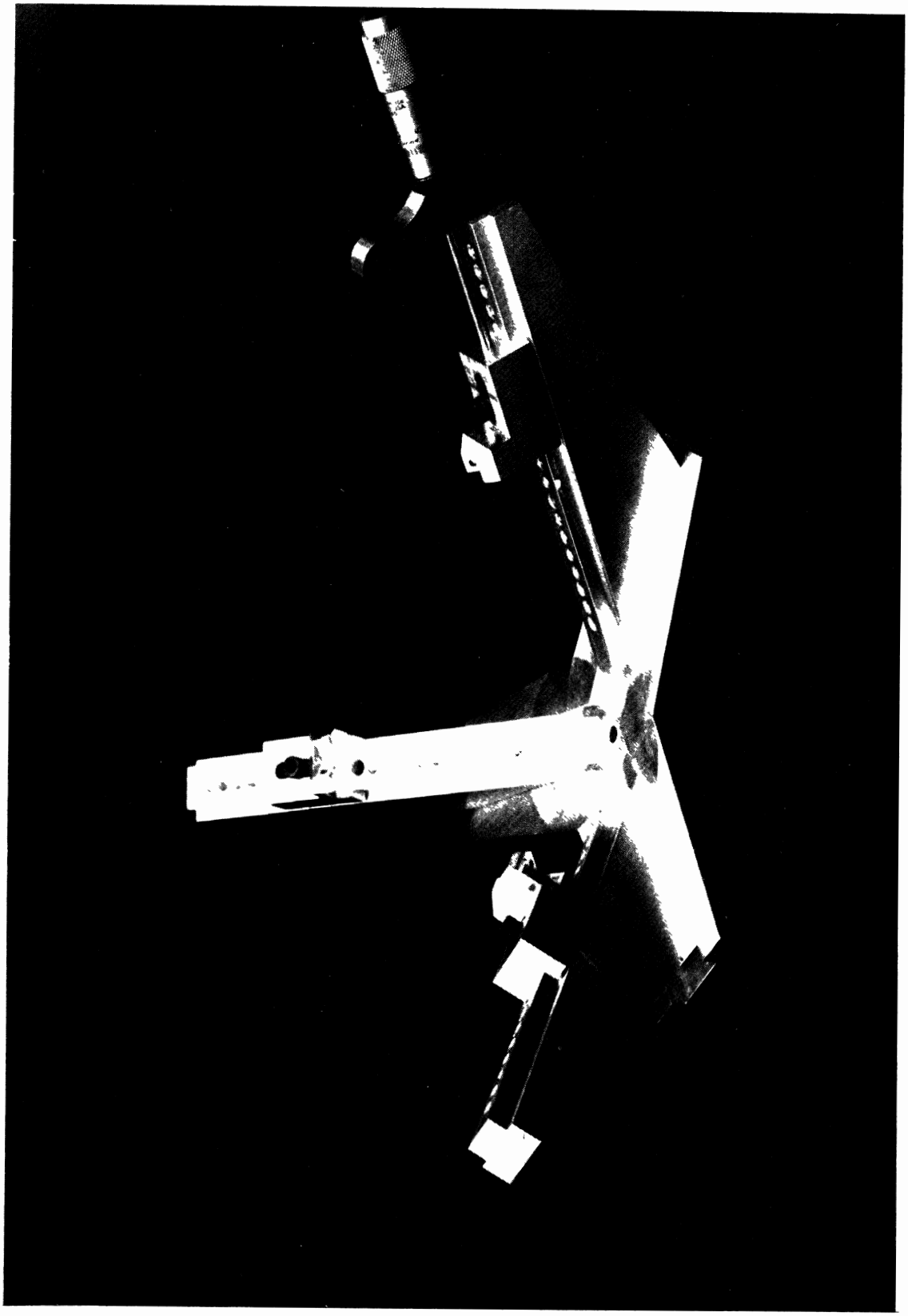

Figure A-6 Accelerometer Location Measurement

7. Insert the collets, thread on and tighten the cups.
8. Remove the pointers from the accelerometer.
9. With the accelerometer mounts still attached to the fixture, insert each mount into its corresponding cup to ensure they fit. It is usually necessary to loosen one of the sliding blocks slightly to accomplish this.
10. Remove the fixture assembly. Fill all the cups with potting material and replace the mounts into the cups as in the previous step. Lock all sliding blocks securely.
11. Measure the distances from the end of each fixture arm to the end of its sliding block and record on the data sheet. See Figure A-6.
12. When the potting material has hardened, remove the screws holding the accelerometer mounts to the sliding blocks, and loosen at least one of the sliding blocks. Remove the fixture from the head.
13. Install the dummy blocks on the accelerometer mounts. These blocks have a lead pellet at the effective center of mass of each accelerometer pair and are used in the x-ray analysis of accelerometer orientation.
14. After x-rays have been taken, remove dummy blocks and install accelerometers. Complete data sheet identifying each accelerometer and its position according to Figure A-3.
15. For movie analysis of accelerometer motion, spherical targets may be provided around each accelerometer pair by attaching a hollowed out styrofoam ball and painting it to contrast with the immediate surroundings. Locate the center of the styrofoam ball at the center of mass of the accelerometer pair.

16. After testing, potting material may be chipped from cup and accelerometer mount and all the pieces reused.

A.4 Three Dimensional X-Ray Technique

In measuring accelerations of points on the head, it is difficult to locate and orient the accelerometers in standard anatomical locations and directions. It is therefore more convenient to resolve quantities measured in an arbitrary coordinate system into components in the standard anatomical directions. All that is needed is an accurate description of the mathematical transformation between the two coordinate systems.

Let $(\hat{e}_1, \hat{e}_2, \hat{e}_3)$ be an arbitrary coordinate system used in instrumenting the head, and let $(\hat{i}, \hat{j}, \hat{k})$ be the standard anatomical coordinate system, commonly referred to as the (A-P), (L-R) and (S-I) axes. Both systems may be termed body-axes triads, which are fixed one relative to the other, but moving with the head. An inertial frame $(\hat{I}, \hat{J}, \hat{K})$ is used as a reference to both moving frames. Then

$$\begin{Bmatrix} \hat{e}_1 \\ \hat{e}_2 \\ \hat{e}_3 \end{Bmatrix} = [E] \begin{Bmatrix} \hat{I} \\ \hat{J} \\ \hat{K} \end{Bmatrix} \tag{1}$$

and

$$\begin{Bmatrix} \hat{i} \\ \hat{j} \\ \hat{k} \end{Bmatrix} = [A] \begin{Bmatrix} \hat{I} \\ \hat{J} \\ \hat{K} \end{Bmatrix} \tag{2}$$

where [E] and [A] are the direction cosines matrix relative to the inertial frame of the instrumentation and the anatomical coordinate systems, respectively.

The objective is to obtain a transformation matrix between $(\hat{e}_1, \hat{e}_2, \hat{e}_3)$ and $(\hat{i}, \hat{j}, \hat{k})$:

$$\begin{Bmatrix} \hat{e}_1 \\ \hat{e}_2 \\ \hat{e}_3 \end{Bmatrix} = [R] \begin{Bmatrix} \hat{i} \\ \hat{j} \\ \hat{k} \end{Bmatrix} \tag{3}$$

From (2), an expression for $(\hat{I}, \hat{J}, \hat{K})$ is obtained:

$$\begin{Bmatrix} \hat{I} \\ \hat{J} \\ \hat{K} \end{Bmatrix} = [A]^{-1} \begin{Bmatrix} \hat{i} \\ \hat{j} \\ \hat{k} \end{Bmatrix} \tag{4}$$

Equation (4) is then substituted into equation (1)

$$\begin{Bmatrix} \hat{e}_1 \\ \hat{e}_2 \\ \hat{e}_3 \end{Bmatrix} = [E]\,[A]^{-1} \begin{Bmatrix} \hat{i} \\ \hat{j} \\ \hat{k} \end{Bmatrix} \tag{5}$$

By comparing equations (3) and (5):

$$[R] = [E][A]^{-1} \tag{6}$$

A.4.1 Method

To obtain [R], one must obtain [E] and [A] which involve the following steps:

a. define $(\hat{e}_1, \hat{e}_2, \hat{e}_3)$

b. define $(\hat{i}, \hat{j}, \hat{k})$

c. devise a method to compute the direction cosine matrix [E] of $(\hat{e}_1, \hat{e}_2, \hat{e}_3)$ relative to an arbitrary inertial frame.

d. devise a method to compute the direction cosine matrix [A] of $(\hat{i}, \hat{j}, \hat{k})$ relative to the same arbitrary inertial frame.

e. compute the matrix product $[E]\,[A]^{-1}$ to obtain the direction cosines matrix [R] of $(\hat{e}_1, \hat{e}_2, \hat{e}_3)$ relative to $(\hat{i}, \hat{j}, \hat{k})$.

A.4.2 Definitions

Instrumentation Definitions - The configuration of the 6 accelerometers necessary to measure the head motion was chosen so that they lie on the 3 axes of the instrumentation coordinate system. Each pair is located at a known distance from the origin P of this system as in Figure A-7. Thus:

$$\overrightarrow{PQ}_1 = \rho_1 \hat{e}_1 \Rightarrow \hat{e}_1 = \frac{\overrightarrow{PQ}_1}{|PQ_1|} \tag{7}$$

$$\overrightarrow{PQ}_2 = \rho_2 \hat{e}_2 \Rightarrow \hat{e}_2 = \frac{\overrightarrow{PQ}_2}{|PQ_2|} \tag{8}$$

$$\overrightarrow{PQ}_3 = \rho_3 \hat{e}_3 \Rightarrow \hat{e}_3 = \frac{\overrightarrow{PQ}_3}{|PQ_3|} \tag{9}$$

Anatomical Definitions - The standard definition of the (A-P), (L-R) and (S-I) axes, or alternately the $(\hat{i}, \hat{j}, \hat{k})$ system is based on the Frankfort plane. This plane is defined by the four points (see Figure A-8).

P_1 : superior edge of the right auditory meatus,

P_2 : superior edge of the left auditory meatus,

P_3 : right infraorbital notch, and

P_4 : left infraorbital notch.

Let C be the midpoint between P_1 and P_2, and M the mid-point between P_3 and P_4, then

a. the anatomical center is defined as point C

b. the A-P axis is defined as:

$$\hat{i} = \frac{\overrightarrow{CM}}{|CM|} \tag{10}$$

c. the L-R axis is defined as:

$$\hat{j} = \frac{\overrightarrow{CP}_2}{|CP_2|} \tag{11}$$

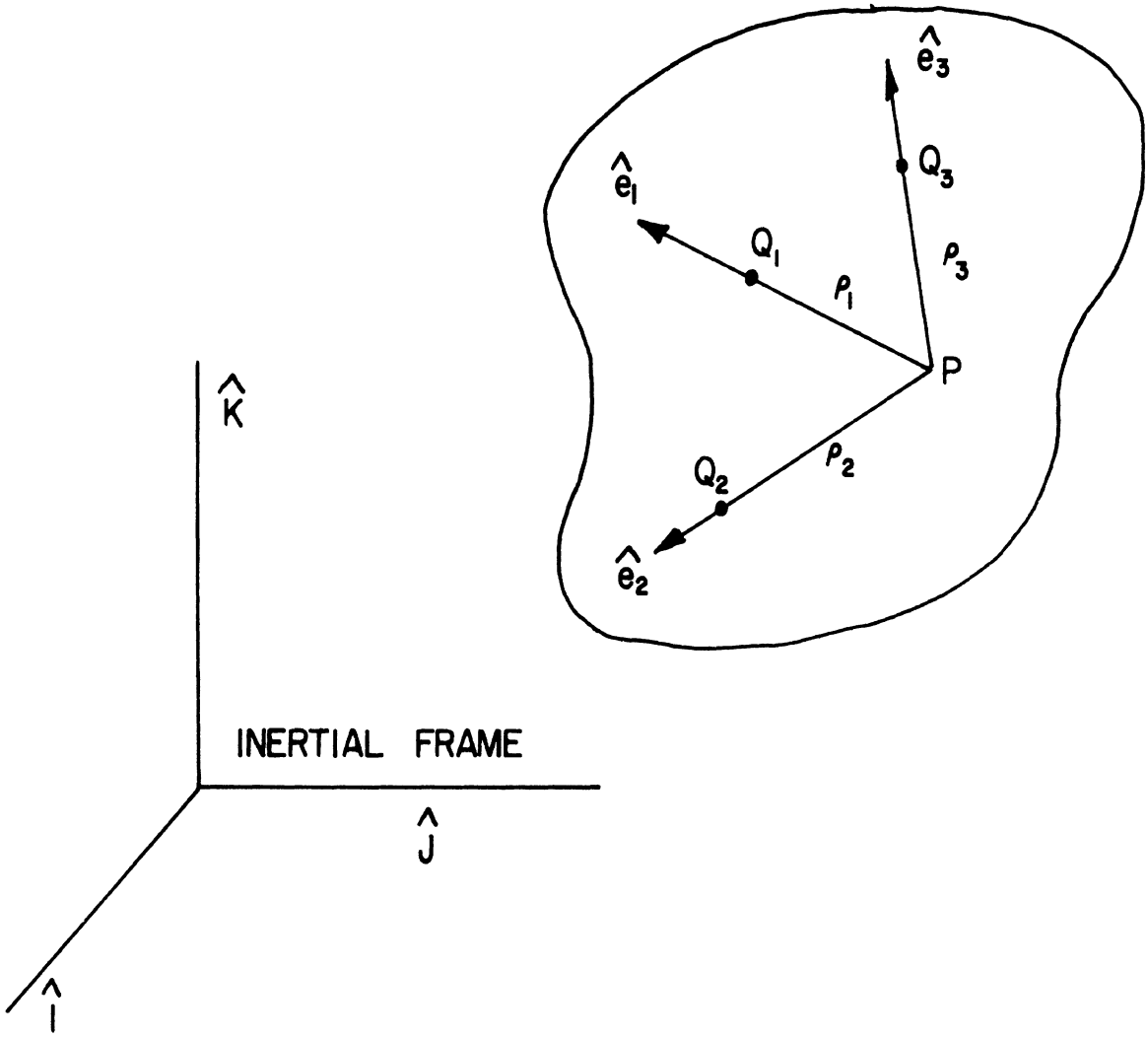

FIGURE A-7: INSTRUMENTATION COORDINATE SYSTEM FOR THE HEAD.

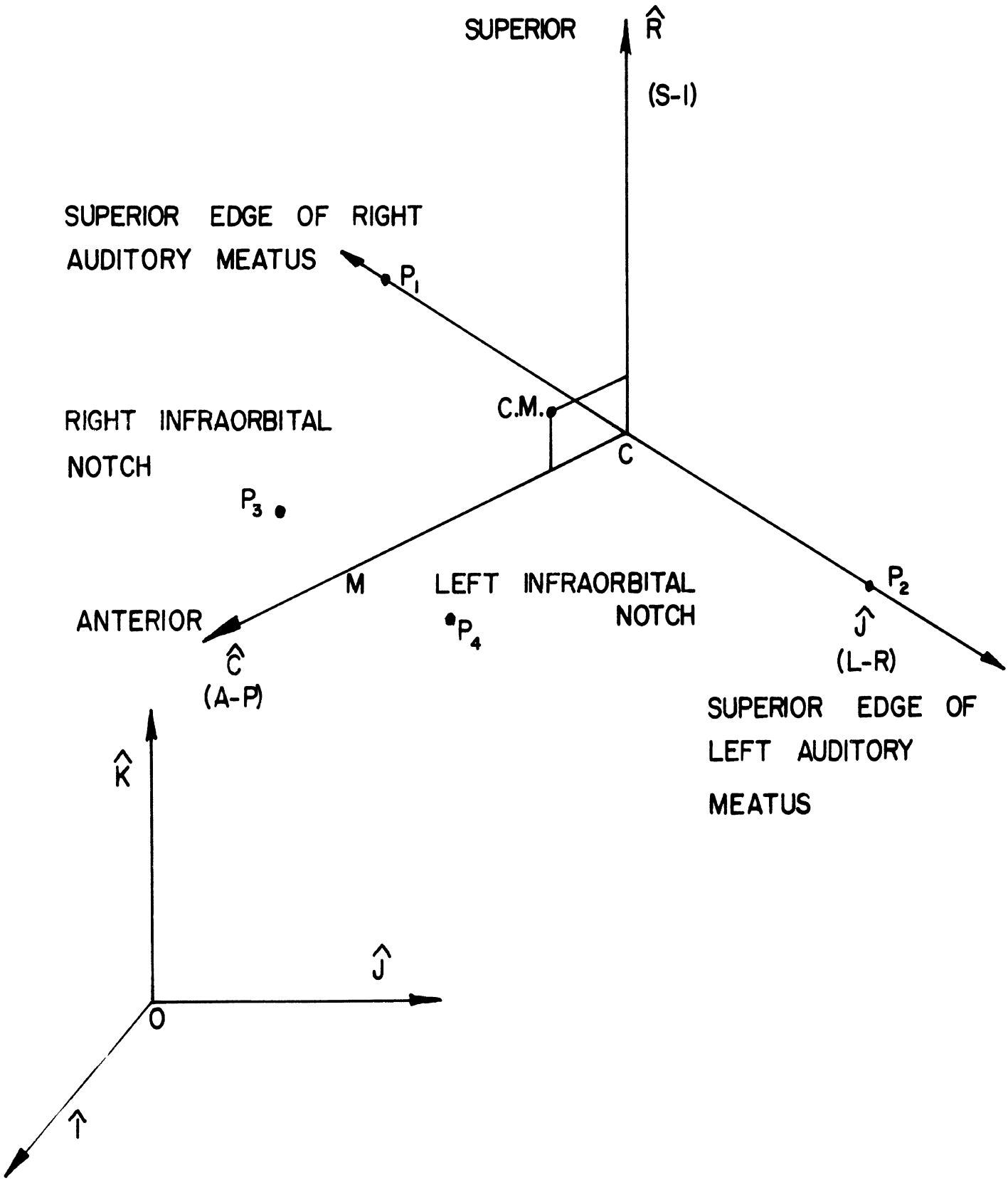

FIGURE A-8: ANATOMICAL POINTS DEFINING THE FRANKFORT PLANE.

d. the S-I axis is defined by the cross product

$$\hat{k} = \hat{i} \times \hat{j} \tag{12}$$

A.4.3 X-Ray Measurements of a Single Point

Two-dimensional coordinates - The x-ray photograph of an object is simply the shadow of that object captured on a photo-sensitive film and generated by a near-point source of x-rays.

It is proposed to obtain the true coordinates (x,z) of an object (see Figure A-9) given the x-ray photo itself, and relevant characteristics of the x-ray set-up which produced it.

A typical x-ray set-up is simplified in the diagram of figure A-9. The x-ray table is vertical in this case, and the film cassette is located behind the table at a distance B. The distance between the table and the x-ray source is A, and between the table and the object is D. After the film has been developed, the trace O of the optical axis is physically located on the film and the distances X and Z are measured.

Given the measured X and Z, the radial distance R and the angle θ may be computed:

$$R = \sqrt{X^2 + Z^2} \tag{13}$$

$$\theta = \tan^{-1}\left[\frac{Z}{X}\right] \tag{14}$$

Now the true radial distance r may be obtained from the geometrical property:

$$\frac{r}{R} = \frac{A-D}{A+B} = \left(\frac{A}{A+B}\right) - \left(\frac{1}{A+B}\right) D \tag{15}$$

or

$$r = [\alpha - \beta D]R \tag{16}$$

The constants α and β depend solely on the x-ray set-up and are the same for any object at any distance D from the x-ray table.

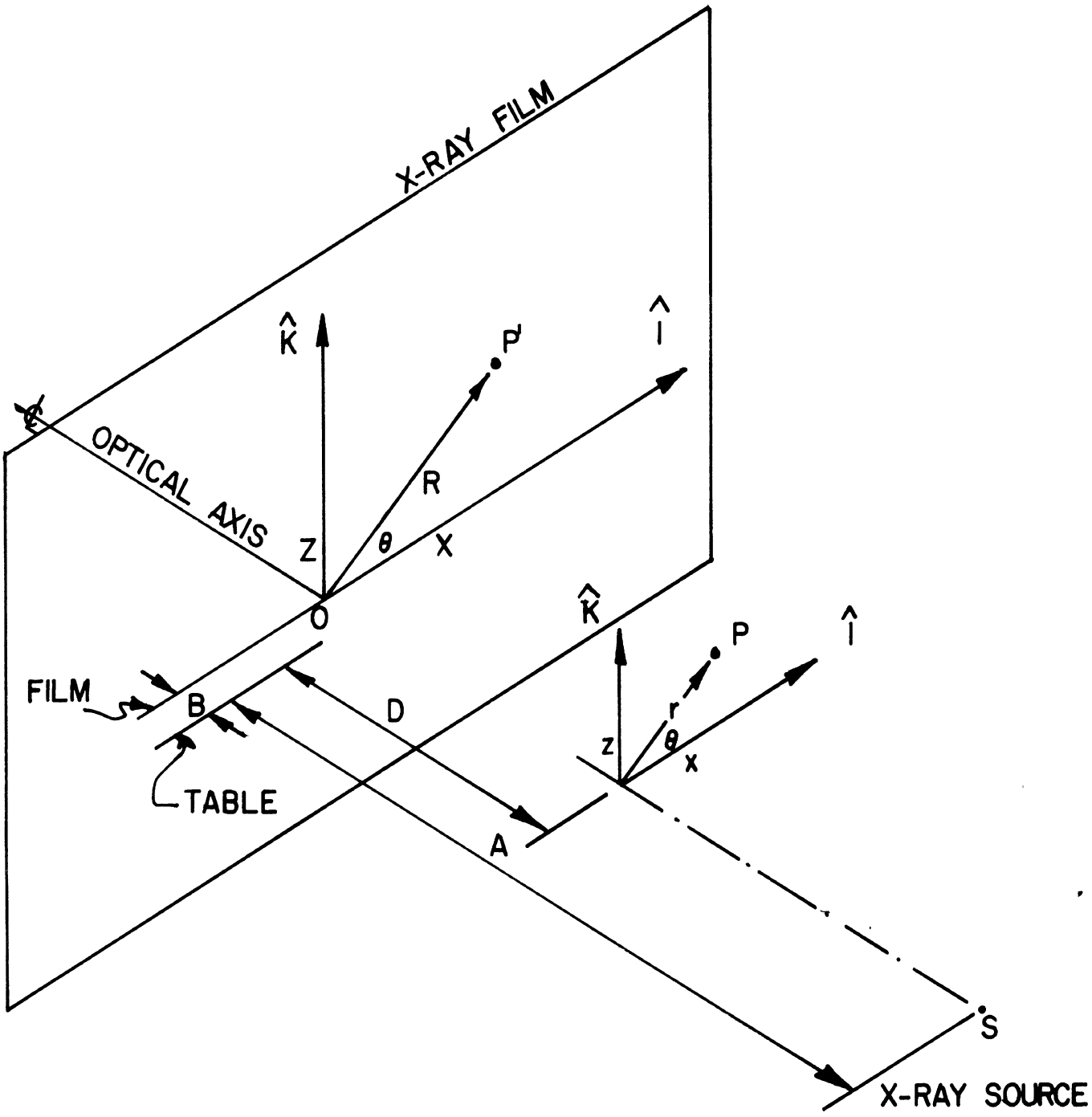

FIGURE A-9: SIMPLIFIED X-RAY SET-UP FOR A SINGLE POINT

The relationship of equation (16) was experimentally determined and is shown in figure A-10. Note that this parametric calibration curve is valid for the x-ray set-up at HSRI and will vary depending on the A and B distances.

Now that the true radial distance is known, the true coordinates are:

$$x = r \cos\theta \tag{17}$$

$$z = r \sin\theta \tag{18}$$

Three-dimensional coordinates - To obtain complete 3-D coordinates of an object point, the procedure followed in the previous section may be repeated for the (Y-Z) plane. This can be done simultaneously with the (X-Z) measurement which requires two separate x-ray sources and two separate film planes, which are mutually perpendicular. A simpler method is to x-ray the (X-Z) plane first, then rotate the object 90° and obtain a new x-ray which would be of the (Y-Z) plane. The analysis of the two x-rays would yield true (x,z) and (y,z) coordinates. The z-coordinate would be the average of the two values obtained, since experimental errors would normally result in slightly different values.

The inertial coordinate reference system is formed by the optical axis going once through the (x,z) plane, then going again through the (y,z) plane of the head. Therefore, care must be taken as to keep the head at the same elevation with respect to the optical axis when it is being rotated. This elevation may, however, be arbitrary.

A.4.4 Experimental X-Ray Procedure

The experimental procedure in x-raying the head must be oriented toward an accurate measurement of the transformation matrix between the instrumentation and the anatomical coordinate system. This procedure is described and justified in the following paragraphs.

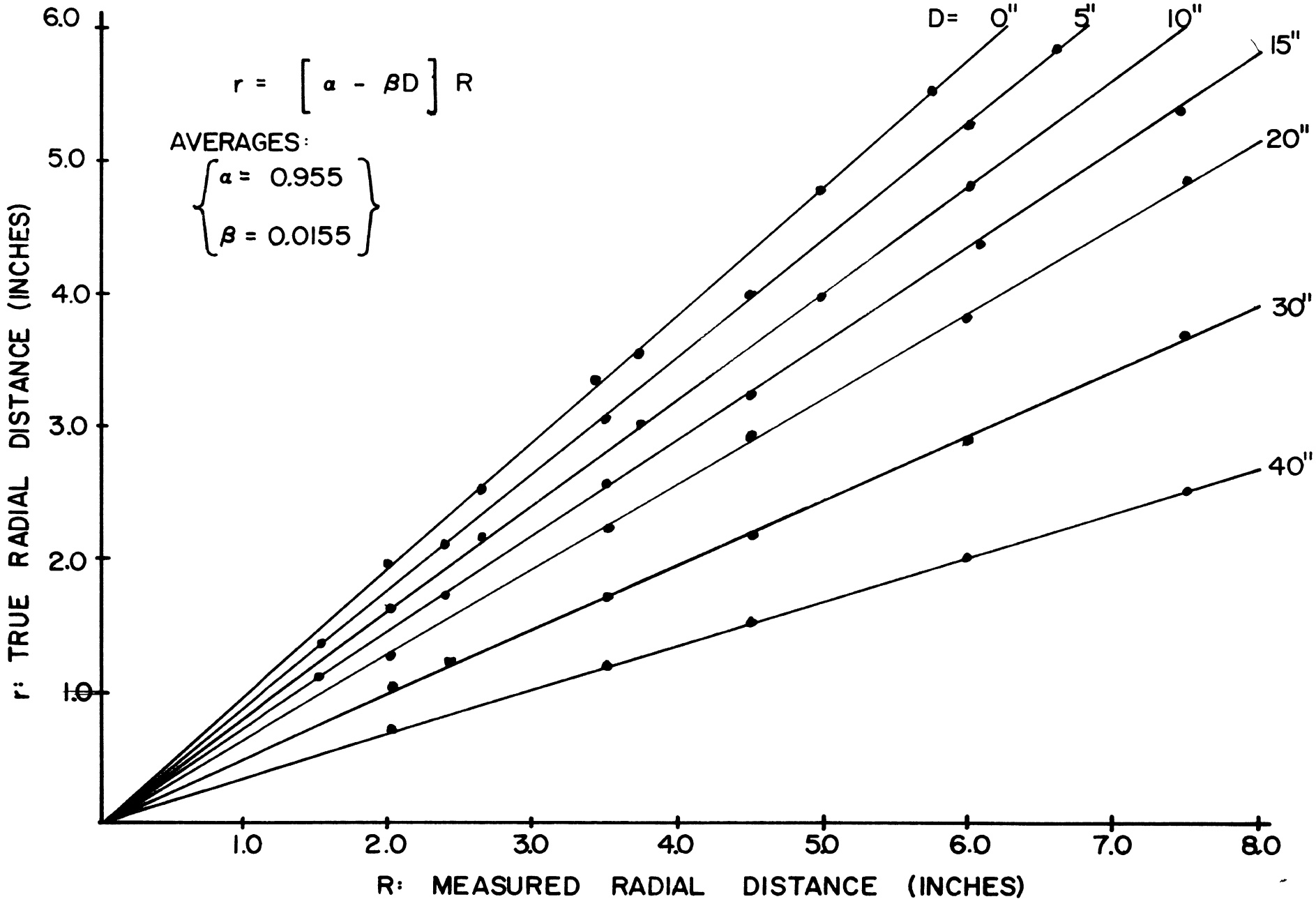

FIGURE A-10: CALIBRATION OF X-RAY SET-UP

On each x-ray, the optical (inertial) reference frame must be defined. For this purpose, a special lead plate, figure A-11, was machined to fit precisely over the window of the x-ray source. This plate will allow a thin circular ring of x-rays to pass through and be recorded on the film, prior to taking the x-ray of the head. Careful machining insures that the optical center is the same as the center of the ring. A vertical axis was obtained on the film by hanging a weight from a long lead wire and taping the top end of the wire onto the x-ray table. Thus, the optical center, as well as the vertical and horizontal optical axes may accurately be drawn on the film and used to measure the (X, Y, Z) coordinates of any given point.

In order to identify the 4 anatomical points of the Frankfort plane, lead pellets with distinctive tabs are used as follows. The lowest points on the two orbital cavities are exposed by small incisions and, using Eastman-910 cement, two pellets are cemented directly on the bone at the lowest point of each orbital cavity. This is the closest approximation to the two infraorbital notches P_3 and P_4 used in defining the Frankfort plane. To approximate the other two points of this plane, P_1 and P_2, two wooden plugs (short cylinders) are used to carry lead pellets so that, when these plugs are inserted in the auditory meati, the lead pellets would approximate the superior edges of the two meati.

Finally, to identify the 3 points Q_1, Q_2, Q_3 which represent the centers of mass of the 3 pairs of accelerometers, 3 aluminum dummy blocks are machined to replace the 3 pairs of accelerometers during the x-raying. Each dummy block contains a pellet, so located as to precisely fall on the c.m. of the accelerometer-pair which is being replaced.

Once the seven pellets are properly mounted on the head, the subject whose head is being x-rayed is then placed (or seated) on a rolling chair

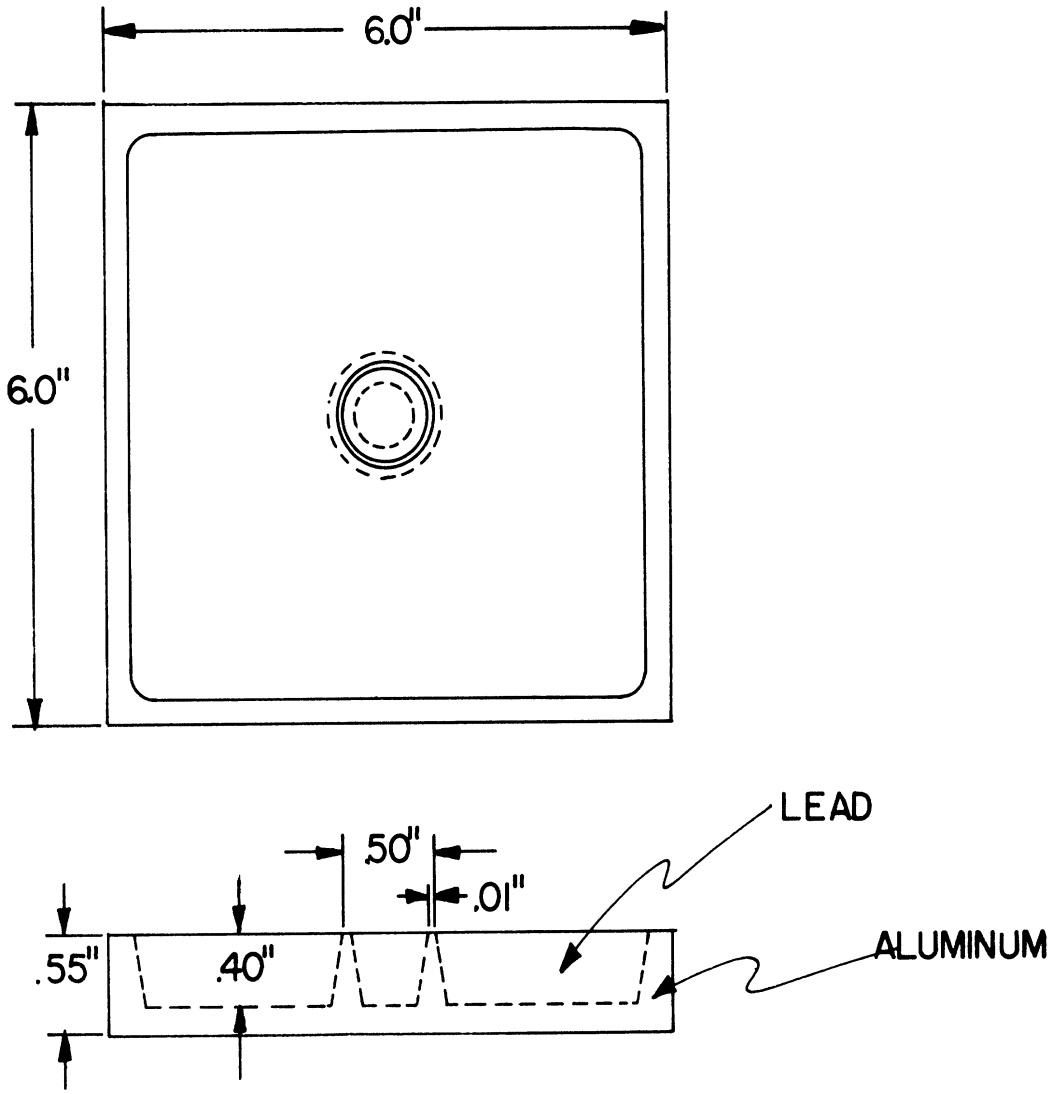

FIGURE A-11: LEAD PLATE FOR PRE-RECORDING OF OPTICAL CENTER.

or platform and the following steps are taken:

Step 1. With the subject outside the x-ray field, expose the film with the circular ring.

Step 2. Place the subject in the x-ray field, and obtain and record the distances of seven pellets from the x-ray table.

Step 3. Expose the film to obtain the x-ray of the head structure and the vertical lead wire. This gives the x-ray of the $(\hat{J}\text{-}\hat{K})$ plane.

Step 4. Remove the subject from the x-ray field, and change the film cassette.

Step 5. Expose the film to obtain the circular ring.

Step 6. Replace the subject to exactly the same previous elevation and in the x-ray field.

Step 7. Rotate the platform carrying the subject through +90° about the $\hat{K}$-axis.

Step 8. Obtain and record the seven distances between the x-ray table and the individual pellets.

Step 9. Expose the head and the vertical lead wire to obtain an x-ray of the $(\hat{X},\hat{K})$ plane.

Once the two orthogonal x-rays have been developed, the optical center and axes are drawn and the seven pellets labeled on each x-ray, then for each pellet, (X,Z) and (Y,Z) pairs are measured directly from the x-rays. These pairs are supplemented with the corresponding distances from the x-ray table obtained earlier during steps 2 and 8 of the x-raying procedure. Each pellet will then have (X, Z, D_{xz}) and (Y,Z,D_{yz}) which can be used to obtain true (x,y,z) coordinates with respect to an arbitrary reference frame, given the calibration constants α and β of the x-ray set-up.

A.4.5 Computational Procedure

A computer program, XRAY, was written to carry the necessary steps toward the evaluation of the transformation matrix [R] between the instrumentation and the anatomical coordinate systems.

Instrumentation Frame - The inertial vector position of the 3 accelerometer pellets may be obtained:

$$\begin{aligned} \overrightarrow{OQ}_1 &= x_1 \hat{I} + y_1 \hat{J} + z_1 \hat{K} \\ \overrightarrow{OQ}_2 &= x_2 \hat{I} + y_2 \hat{J} + z_2 \hat{K} \\ \overrightarrow{OQ}_3 &= x_3 \hat{I} + y_3 \hat{J} + z_3 \hat{K} \end{aligned} \tag{19}$$

and

$$\overrightarrow{OP} = x_p \hat{I} + y_p \hat{J} + z_p \hat{K}$$

But

$$\begin{aligned} \overrightarrow{OP}_1 &= \overrightarrow{OP} + \overrightarrow{PQ}_1 \\ \overrightarrow{OQ}_2 &= \overrightarrow{OP} + \overrightarrow{PQ}_2 \\ \overrightarrow{OQ}_3 &= \overrightarrow{OP} + \overrightarrow{PQ}_3 \end{aligned} \tag{20}$$

where

$$\begin{aligned} \overrightarrow{PQ}_1 &= \rho_1 \hat{e}_1 \\ \overrightarrow{PQ}_2 &= \rho_2 \hat{e}_2 \\ \overrightarrow{PQ}_3 &= \rho_3 \hat{e}_3 \end{aligned} \tag{21}$$

The first step in solving the problem is to obtain the inertial coordinates of point P, origin of the instrumentation triad. Solving for $\overrightarrow{PQ}_1$, $\overrightarrow{PQ}_2$ and $\overrightarrow{PQ}_3$ from equation (20) and substituting the values in equation (21) yields:

$$\begin{aligned} \rho_1 \hat{e}_1 &= \overrightarrow{OQ}_1 - \overrightarrow{OP} = (x_1 - x_p)\hat{I} + (y_1 - y_p)\hat{J} + (z_1 - z_p)\hat{K} \\ \rho_2 \hat{e}_2 &= \overrightarrow{OQ}_2 - \overrightarrow{OP} = (x_2 - x_p)\hat{I} + (y_2 - y_p)\hat{J} + (z_3 - z_p)\hat{K} \\ \rho_3 \hat{e}_3 &= \overrightarrow{OQ}_3 - \overrightarrow{OP} = (x_3 - x_p)\hat{I} + (y_3 - y_p)\hat{J} + (z_3 - z_p)\hat{K} \end{aligned} \tag{22}$$

Equations (22) may be written in scalar form by dot multiplying each equation by itself:

$$\begin{aligned}
\rho_1^2 &= (x_1-x_p)^2+ (y_1-y_p)^2+ (z_1- z_p)^2 \\
\rho_2^2 &= (x_2-x_p)^2+ (y_2-y_p)^2+ (z_2- z_p)^2 \\
\rho_3^2 &= (x_3-x_p)^2+ (y_3-y_p)^2+ (z_3- z_p)^2
\end{aligned} \tag{23}$$

Equations (23) may be manipulated to obtain the following linear simultaneous equations:

$$\begin{bmatrix} (x_1-x_2) & (y_1-y_2) & (z_1-z_2) \\ (x_2-x_3) & (y_2-y_3) & (z_2-z_3) \\ (x_3-x_1) & (y_3-y_1) & (z_3-z_1) \end{bmatrix} \begin{Bmatrix} x_p \\ y_p \\ z_p \end{Bmatrix} \begin{Bmatrix} (x_1^2+ y_1^2+ z_1^2-\rho_1^2)-(x_2^2+ y_2^2+ z_2^2-\rho_2^2) \\ (x_2^2+ y_2^2+ z_2^2-\rho_2^2)-(x_3^2+ y_3^2+ z_3^2-\rho_3^2) \\ (x_3^2+ y_3^2+ z_3^2-\rho_3^2)-(x_3^2+ y_3^2+ z_3^2-\rho_3^2) \end{Bmatrix} \tag{24}$$

Finally this set of equations is solved by subroutine LOCOR to yield $(x_p, y_p z_p)$. The next step is simple and involves computing the direction cosines of each of the vectors $\vec{PQ}_1$, $\vec{PQ}_2$, $\vec{PQ}_3$ which are identical with those of the unit vectors $\hat{e}_1$, $\hat{e}_2$, $\hat{e}_3$. Thus:

$$\begin{aligned}
\hat{e}_1 &= \frac{\vec{PQ}_1}{|PQ_1|} = \frac{x_1-x_p}{\rho_1}\hat{I} + \frac{y_1-y_p}{\rho_1}\hat{J} + \frac{z_1- z_p}{\rho_1}\hat{K} \\
\hat{e}_2 &= \frac{\vec{PQ}_2}{|PQ_2|} = \frac{x_2- x_p}{\rho_2}\hat{I} + \frac{y_2-y_p}{\rho_2}\hat{J} + \frac{z_2-z_p}{\rho_2}\hat{K} \\
\hat{e}_3 &= \frac{\vec{PQ}_3}{|PQ_3|} = \frac{x_3-x_p}{\rho_3}\hat{I} + \frac{y_3-y_p}{\rho_3}\hat{J} + \frac{z_3-z_p}{\rho_3}\hat{K}
\end{aligned} \tag{25}$$

or simply

$$\begin{Bmatrix} \hat{e}_1 \\ \hat{e}_2 \\ \hat{e}_3 \end{Bmatrix} = [E] \begin{Bmatrix} \hat{I}_1 \\ \hat{J}_2 \\ \hat{K}_3 \end{Bmatrix} \tag{26}$$

Anatomical Frame - Using the same notation for the anatomical pellets, the inertial position vectors of the four anatomical pellets are:

$$\begin{aligned}
\overrightarrow{OP}_1 &= x_1\hat{I} + y_1\hat{J} + z_1\hat{K} \\
\overrightarrow{OP}_2 &= x_2\hat{I} + y_2\hat{J} + z_2\hat{K} \\
\overrightarrow{OP}_3 &= x_3\hat{I} + y_3\hat{J} + z_3\hat{K} \\
\overrightarrow{OP}_4 &= x_4\hat{I} + y_4\hat{J} + z_4\hat{K}
\end{aligned} \tag{27}$$

First define the direction cosines of $\hat{j}$-axis or the L-R axis. This may be done by one of two methods:

$$\hat{j} = \frac{\overrightarrow{P_1P_2}}{|\overrightarrow{P_1P_2}|} = \ell_1\hat{I} + m_1\hat{J} + n_1\hat{K}$$

or

$$\hat{j} = \frac{\overrightarrow{P_3P_4}}{|\overrightarrow{P_3P_4}|} = \ell_2\hat{I} + m_2\hat{J} + n_2\hat{K}$$

The two methods are equivalent within some experimental error. To minimize this error, the average is taken as the final direction cosines of unit vector $\hat{j}$, i.e.:

$$\hat{j} = \frac{\ell_1+\ell_2}{2}\hat{I} + \frac{m_1+m_2}{2}\hat{J} + \frac{n_1+n_2}{2}\hat{K} \tag{28}$$

Next, define the S-I or $\hat{k}$-axis. This axis is perpendicular to the Frankfort plane defined by the 4 anatomical pellets. The unit vector $\hat{k}$ must be along the cross product of the vector $\hat{j}$ and any vector $\vec{P}$ lying in the Frankfort plane. Thus:

$$\hat{k} = \frac{\hat{j} \times \overrightarrow{P_3P_1}}{|\hat{j} \times \overrightarrow{P_3P_1}|} = \ell_1\hat{I} + m_1\hat{J} + n_1\hat{K}$$

or $$\hat{k} = \frac{\hat{j} \times \overrightarrow{P_4P_1}}{|\hat{j} \times \overrightarrow{P_4P_1}|} = \ell_2\hat{I} + m_2\hat{J} + n_2\hat{K}$$

or $$\hat{k} = \frac{\hat{j} \times \overrightarrow{P_3P_2}}{|\hat{j} \times \overrightarrow{P_3P_2}|} = \ell_3\hat{I} + m_3\hat{J} + n_3\hat{K}$$

or $$\hat{k} = \frac{\hat{j} \times \overrightarrow{P_4P_2}}{\hat{j} \times \overrightarrow{P_4P_2}} = \ell_4\hat{I} + m_4\hat{J} + n_4\hat{K}$$

The average is then :

$$\hat{k} = \frac{\ell_1+\ell_2+\ell_3+\ell_4}{4}\ \hat{I} + \frac{m_1+m_2+m_3+m_4}{4}\ \hat{J} + \frac{n_1+n_2+n_3+n_4}{4}\ \hat{K} \qquad (29)$$

Finally, the direction cosines of the A-P or $\hat{i}$-axis are obtained by the cross product:

$$\hat{i} = \hat{k} \times \hat{j} \qquad (30)$$

Equations (28), (29) and (30) may be written compactly as:

$$\begin{Bmatrix} \hat{i} \\ \hat{j} \\ \hat{k} \end{Bmatrix} = [A] \begin{Bmatrix} \hat{I} \\ \hat{J} \\ \hat{K} \end{Bmatrix}$$

Transformation matrix [R] - Since the transformation matrix [R], defined by

$$\begin{Bmatrix} \hat{e}_1 \\ \hat{e}_2 \\ \hat{e}_3 \end{Bmatrix} = [R] \begin{Bmatrix} \hat{i} \\ \hat{j} \\ \hat{k} \end{Bmatrix} ,$$

is the desired result, it is simply obtained by:

$$[R] = [E]\,[A]^{-1}$$

The matrix [A] is an orthogonal transformation, therefore, its inverse is equal to its transpose.

$$[A]^{-1} = [A]^T$$

Thus,

$$[R] = [E]\,[A]^T \qquad (31)$$

The matrix multiplication in Equation (31) is straightforward.

Translation of the two origins - In addition to the transformation matrix between the instrumentation and the anatomical coordinate systems, the location of the instrumentation origin P must be known relative to the anatomical coordinate system, i.e.

$$\overrightarrow{CP} = d_1\,\hat{i} + d_2\,\hat{j} + d_3\,\hat{k}. \tag{32}$$

This vector can be computed from

$$\overrightarrow{CP} = \overrightarrow{OP} - \overrightarrow{OC}$$

then expressed in the anatomical system. First, the vector $\overrightarrow{OC}$ is by definition (section A.4.2)

$$\overrightarrow{OC} = \frac{1}{2}[\overrightarrow{OP}_1 + \overrightarrow{OP}_2]$$

$$\overrightarrow{OC} = \frac{x_1+x_2}{2}\,\hat{I} + \frac{y_1+y_2}{2}\,\hat{J} + \frac{z_1+z_2}{2}\,\hat{K} \tag{33}$$

or $$\overrightarrow{OC} = x_c\,\hat{I} + y_c\,\hat{J} + z_c\,\hat{K}$$

and $$\overrightarrow{OP} = x_p\,\hat{I} + y_p\,\hat{J} + z_p\,\hat{K}$$

therefore $$\overrightarrow{CP} = (x_p-x_c)\,\hat{I} + (y_p-y_c)\,\hat{J} + (z_p-z_c)\,\hat{K} \tag{34}$$

To obtain (d_1, d_2, d_3), the anatomical components of $\overrightarrow{CP}$, we express $\overrightarrow{CP}$ in the anatomical system:

$$\overrightarrow{CP} = \begin{bmatrix}(x_p-x_c) & (y_p-y_c) & (z_p-z_c)\end{bmatrix} \begin{Bmatrix}\hat{I}\\ \hat{J}\\ \hat{K}\end{Bmatrix}$$

Using equation (2), $(\hat{I},\hat{J},\hat{K})$ is substituted to obtain:

$$\begin{bmatrix}d_1 & d_2 & d_3\end{bmatrix} = \begin{bmatrix}(x_p-x_c) & (y_p-y_c) & (z_p-z_c)\end{bmatrix} [A]^T \tag{35}$$

APPENDIX B

CADAVER CHAIR

APPENDIX B CADAVER CHAIR

Problem: Design an apparatus to accurately position a cadaver's head or leg in front of an impacting ram used to study human head and leg impact characteristics. Such a "cadaver seat" would also provide a degree of uniformity in tests of different specimens.

The seat should allow the cadaver's head or leg to recoil natrually from the impacting blow and not restrain the reaction. Impacts to be considered are (1) head frontal, (2) head side, and (3) leg frontal.

Design: A photo of the basic seat is shown in Figure B1. The outer box-like framework sits on the laboratory floor in front of the impactor. Its upper framework structure is used for mounting photographic equipment and other instrumentation. The seat is shown schematically in Figure B-2.

Two sets of rails support the seat within this framework and are arranged so as to provide initial positioning of the seat within the structure in both the vertical and anterior-posterior directions. The seat bottom is mounted to one rail set via four automotive-type power seat tracks (not shown in Figure B1). They are arranged so as to remotely control the fine positioning of the seat with respect to the outer frame and to provide five additional adjustments:

(1) 6" total anterior-posterior translation

(2) 6" total left-right translation

(3) 6" total superior-inferior translation

(4) ±6 1/2° anterior-posterior tilt

(5) ±6 1/2° left-right tilt.

The cadaver is strapped into the seat at the thighs and upper arms and the head is held off the shoulders by strings tied from the ears to a seat member above. Upon frontal/side impact, the string breaks and allows the head to recoil quite naturally. The upper arms are fastened securely

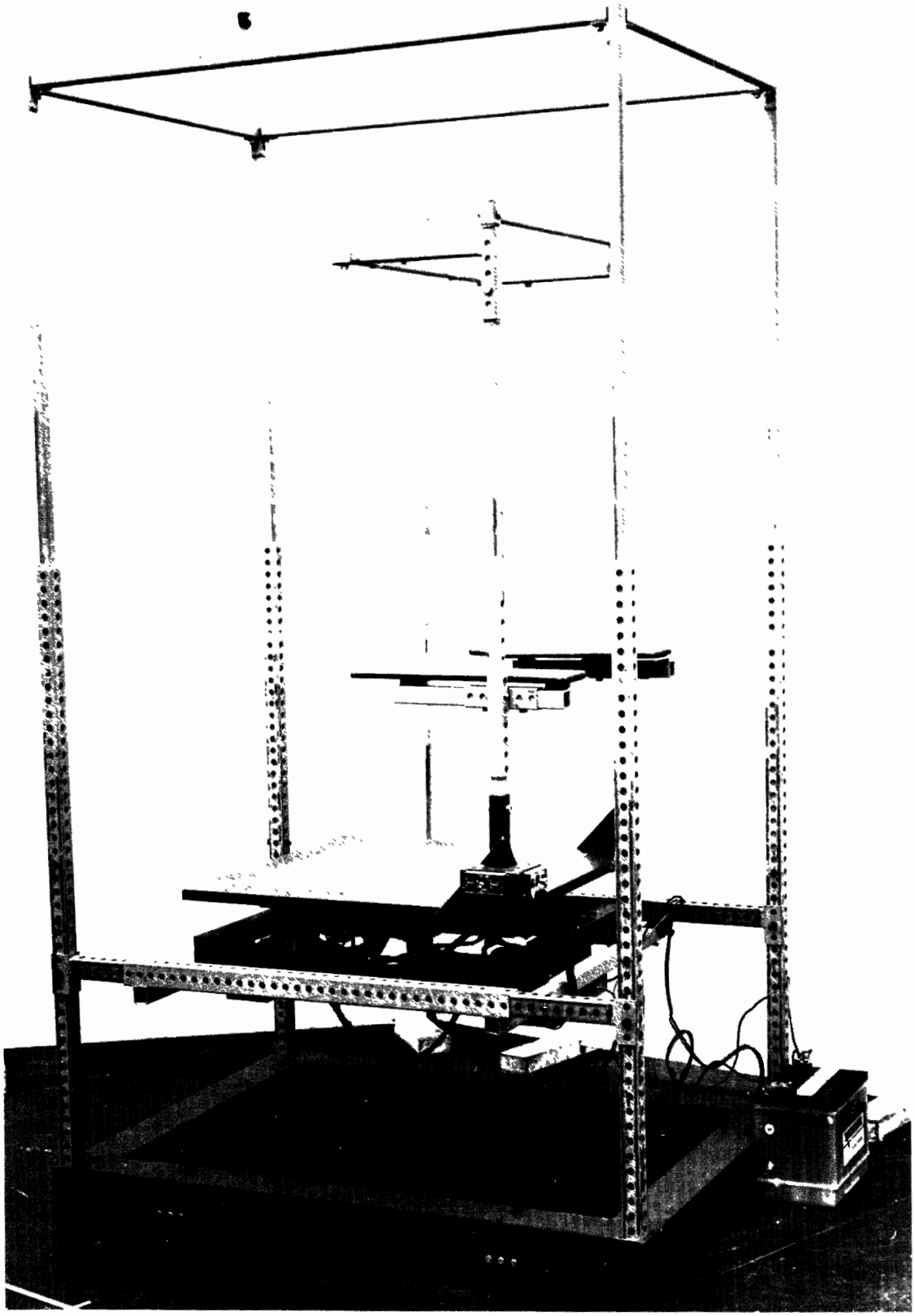

Figure B-1. Cadaver Seat

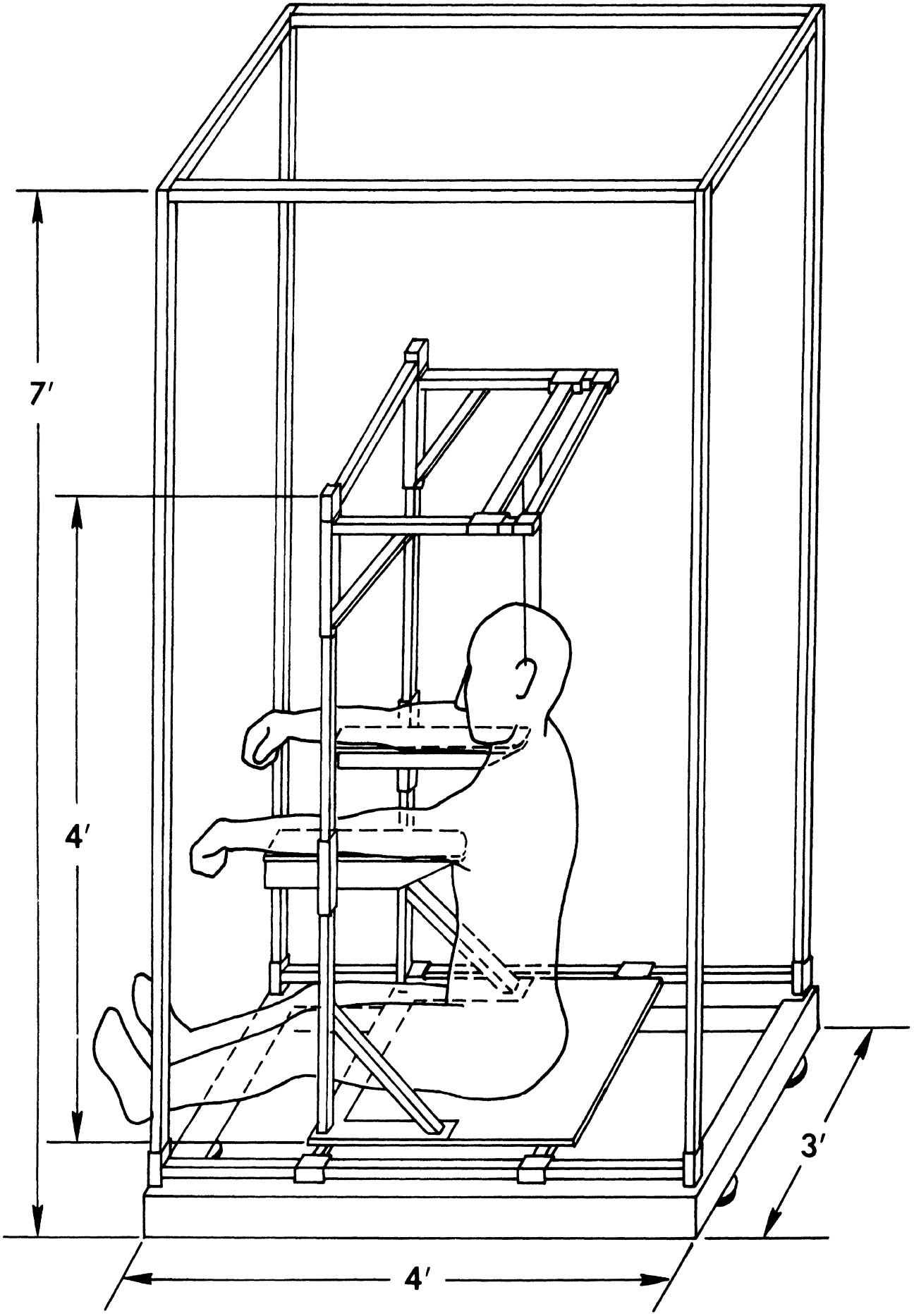

Figure B-2. Cadaver Seat Schematic

enough to hold the torso upright and yet will not significantly restrict posterior chest movement upon frontal chest impact.

APPENDIX C

ANTHROPOMETRY DATA

DATE _____ SUBJECT NO. VRIC-03

CADAVER NO. _____

VRIC ANTHROPOMETRY SHEET

I. SUPINE

CA	1.	Head breadth	14.7
CA	2.	Head length	19.0
RA	3.	Head height	13.5
ST	4.	Sagittal arc length	36.8
ST	5.	Coronal arc length	35.0
RA	6.	Femur length - R	37.0
RA	7.	Femur length - L	39.1

II. CIRCUMFERENCE

ST	1.	Neck (at mid-line)	39.3
ST	2.	Head	57.3

III. STATURE 179.2

CA = Curved anthropometer
RA = Regular anthropometer
ST = Steel tape

RA	8.	Lower leg length - R (Fibula Length)	46.2
RA	9.	Lower leg length - L (Fibula Length)	45.7

Rev. 5/8/74

DATE April 24, 1974 SUBJECT NO. VRIC-04

CADAVER NO. _____

VRIC ANTHROPOMETRY SHEET

I. SUPINE

CA	1.	Head breadth	15.4
CA	2.	Head length	18.0
RA	3.	Head height	12.6
ST	4.	Sagittal arc length	37.0
ST	5.	Coronal arc length	35.8
RA	6.	Femur length - R (upper leg)	
RA	7.	Femur length - L (upper leg)	
RA	8.	Fibula length - R (lower leg)	43.5
RA	9.	Fibula length - L (lower leg)	42.2

II. CIRCUMFERENCE

ST	1.	Neck (at mid-line)	32.5
ST	2.	Head	55.2

CA = Curved anthropometer
RA = Regular anthropometer
ST = Steel tape

Rev. 5/8/74

DATE April 24, 1974 SUBJECT NO. VRIC-04

CADAVER NO. _____

VRIC ANTHROPOMETRY SHEET

I. SUPINE

CA	1.	Head breadth	15.4
CA	2.	Head length	18.0
RA	3.	Head height	12.6
ST	4.	Sagittal arc length	37.0
ST	5.	Coronal arc length	35.8
RA	6.	Femur length - R (upper leg)	
RA	7.	Femur length - L (upper leg)	
RA	8.	Fibula length - R (lower leg)	43.5
RA	9.	Fibula length - L (lower leg)	42.2

II. CIRCUMFERENCE

ST	1.	Neck (at mid-line)	32.5
ST	2.	Head	55.2

CA = Curved anthropometer

RA = Regular anthropometer

ST = Steel tape

Rev. 5/8/74

DATE May 7, 1974 SUBJECT NO. VRIC-05

CADAVER NO. 19940

VRIC ANTHROPOMETRY SHEET

I. SUPINE

CA	1.	Head breadth	15.0
CA	2.	Head length	21.0
RA	3.	Head height	13.6
ST	4.	Sagittal arc length	36.4
ST	5.	Coronal arc length	36.0
RA	6.	Femur length - R (upper leg)	31.8
RA	7.	Femur length - L (upper leg)	32.4
RA	8.	Fibula length - R (lower leg)	40.1
RA	9.	Fibula length - L (lower leg)	37.8
RA	10.	Stature	

II. CIRCUMFERENCE

ST	1.	Neck (at mid-line)	38.7
ST	2.	Head	57.9

CA = Curved anthropometer

RA = Regular anthropometer

ST = Steel tape

Rev. 5/8/74

DATE May 7, 1974 SUBJECT NO. VR1C-05

CADAVER NO. 19940

VRIC ANTHROPOMETRY SHEET

I. SUPINE

CA	1.	Head breadth	15.0
CA	2.	Head length	21.0
RA	3.	Head height	13.6
ST	4.	Sagittal arc length	36.4
ST	5.	Coronal arc length	36.0
RA	6.	Femur length - R (upper leg)	31.8
RA	7.	Femur length - L (upper leg)	32.4
RA	8.	Fibula length - R (lower leg)	40.1
RA	9.	Fibula length - L (lower leg)	37.8
RA	10.	Stature	

II. CIRCUMFERENCE

ST	1.	Neck (at mid-line)	38.7
ST	2.	Head	57.9

CA = Curved anthropometer

RA = Regular anthropometer

ST = Steel tape

Rev. 5/8/74